Original Article
Cytochrome P450 family proteins as potential biomarkers for ovarian granulosa cell damage in mice with premature ovarian failure

Jiajia Lin[1], Jiajia Zheng[1], Hu Zhang[1], Jiulin Chen[1], Zhihua Yu[1], Chuan Chen[1], Ying Xiong[3], Te Liu[1,2]

[1]Shanghai Geriatric Institute of Chinese Medicine, Longhua Hospital, Shanghai University of Traditional Chinese Medicine, Shanghai, China; [2]Department of Pathology, Yale UniversitySchool of Medicine, New Haven, USA; [3]Department of Gynaecology and Obestetrics, Xinhua Hospital Affiliated to Shanghai Jiaotong University School of Medicine, Shanghai, China

Abstract: Premature ovarian failure (POF) is the pathological aging of ovarian tissue. We have previously established a cyclophosphamide-induced mouse POF model and found that cyclophosphamide caused significant damage and apoptosis of mouse ovarian granulosa cells (mOGCs). To systematically explore the molecular biologic evidence of cyclophosphamide-induced mOGC damage at the gene transcription level, RNA-Seqwas used to analyse the differences in mOGC transcriptomes between POF and control (PBS) mice. The sequencing results showed that there were 18765 differential transcription genes between the two groups, of which 192 were significantly up-regulated (log2 [POF/PBS] > 2.0) and 116 were significantly down-regulated (log2 [POF/PBS] < -4.0). Kyoto Encyclopedia of Genes and Genomes analysis found that the neuroactive ligand-receptor interaction pathway was significantly up-regulated and metabolic pathways were significantly down-regulated in the POF group. Gene Ontology analysis showed that the expression of plasma membrane, regulation of transcription and ion binding functions were significantly up-regulated in the POF group, while the expression of cell and cell parts, catalytic activity and single-organism process functions were significantly down-regulated. Finally, protein interaction analysis reveals that in the ovarian steroidogenesis pathway, three Cytochrome P450 family proteins-Cyp1a1, Cyp11a1 and Cyp2u1-interact with Fdx1 to form an interactive network. These three proteins were down-regulated in POF cells, suggesting that they are likely direct regulatory targets of cyclophosphamide. RNA-Seq high-throughput screening analysis demonstrated that cyclophosphamide damage to mOGCs was achieved through its impacts on multiple pathways and on the transcription activities of multiple target genes. Among them, the protein network consisting of the cytochrome P450 family Fdx1, Cyp17a1, Cyp11a1 and Cyp2u1 is a potential new biomarker of mOGC damage in POF in mice.

Keywords: Premature ovarian failure, ovarian granulosa cells, cyclophosphamide, RNA sequencing, transcriptomic differences

Introduction

Premature ovarian failure (POF) is a common gynecological disease that causes female infertility [1-4]. The pathological features are amenorrhea, anovulation, absence of mature follicles,significantly increased gonadotropin levels,and significantly decreased estrogen levels in women before the age of 40 [1-4]. The mechanisms of POF are complex and diverse, and genetic factors, endocrine factors, psychological factors, and autoimmune factors can all lead to its occurrence [1-5]. In addition, there is still no efficacious treatment or medicine for

POF [1-4, 6]. Our previous study found that the injection of cyclophosphamide could cause POF in female mice [4, 7, 8] and cyclophosphamide could significantly damage mouse ovarian granulosa cells (mOGCs) [4, 7, 8]. Although we also revealed some mechanisms at the epigenetic level, the regulatory mechanism at the level of the entire genome is not yet clear.

RNA sequencing (RNA-Seq), also known as whole transcriptome shotgun sequencing (WT-SS), uses next-generation sequencing to reveal changes in RNA transcription levels in biologic samples at a particular time point [9-13]. RNA-

Seq is often used to analyse changes in cellular transcripts [9-13]. In particular, it focuses on-alternative splicing and transcription of genes, modification at the post-transcription level, gene fusion, and transcription differences related to single-nucleotide polymorphisms (SN-Ps) and mutations [9-13]. Moreover, RNA-Seq can also be used to define the boundaries of exons and introns of a gene as well as the boundaries of the previously annotated 5' and 3' ends [9-13]. At present, RNA-Seq has been widely used in the field of genomic regulation in embryonic development, disease mechanisms and screening of drug resistance genes [9-13].

Ferredoxin 1 (Fdx1), an iron-sulfur protein, is a mono-oxygenase that promotes cytochrome P450 enzymatic reactions. The gene encodes a protein that resides in the mitochondrial matrix, and ferredoxin reductase transfers electrons to mitochondrial cytochrome P450. There are multiple Fdx1transcripts encoding different subtypes due to alternative splicing. Fdx1 is highly expressed in adult adrenal glands and ovaries [14-19]. Cyp2u1, which encodes polypeptide 1 of subfamily u in the cytochrome P450 family 2, Cyp11a1, which encodes polypeptide 1 of subfamily a in the cytochrome P450 family 11, and Cyp17a1, which encodes polypeptide 1 of subfamily a in the cytochrome P450 family 17, all belong to the cytochrome P450 family [20]. Tissue distribution of these three genes shows a significant preference, mostly in the ovary, testis, and adrenal gland [20]. Cytochrome P450 (Cyp) represents a large family of self-oxidizing heme proteinsand is a class of mono-oxygenases, named for its specific absorption at 450 nm [20, 21]. It participates in the metabolism of endogenous substances and exogenous substances, including drugs and environmental compounds. According to the degree of homology of the amino acid sequence, its members are divided into the three levels of enzymes: family, subfamily and individual [20, 21]. In cells, Cyp is mainly distributed in the endoplasmic reticulum and the mitochondrial inner membrane, and it acts as a terminal oxygenase to participate in the synthesis of steroid hormones in the body [20, 21]. However, the relationship between the members of the cytochrome P450 enzyme family and the development of POF is still unclear.

To systematically explore the molecular biology evidence of cyclophosphamide-inducedmOGC damage at the transcriptome level and to exploit the related biomarkers, we used RNA-Seq technology to analyse the differences inmOGC transcriptomesbetween mice in the POF group and control group (PBS).

Material and methods

Establishment of a mouse model of POF

Briefly [8], 10-week-old female C57BL/6 mice (n = 6) were purchased from the Experimental Animal Center of Shanghai University of Traditional Chinese Medicine, China. Mice were randomized into two groups,with three mice in each group. POF mice were first injected intraperitoneally with cyclophosphamide at 70 mg/kg (Sigma-Aldrich, St Louis, USA), followed by intraperitoneal injection of cyclophosphamide at 30 mg/kg once every 2 days for 3 consecutive weeks, to construct the POF mouse model. In addition, the control group mice were injected intraperitoneally with the same amount of PBS once every 2 days for 3 consecutive weeks. The study was approved by the Ethics Committee at the Shanghai Institute of Geriatrics (SHAGESYDW2017008). All experiments are in line with China National Science and Technology Commission animal laboratory regulations.

Isolation and culture of OGCs and establishment of the in vitro injury model

Briefly [8], 10-week-old female C57BL/6 mice (n = 10) were purchased from the Experimental Animal Center of Shanghai University of Traditional Chinese Medicine. Mice were euthanized by cervical dislocation, and ovarian tissues were isolated in sterile conditions and placed in PBS at 4°C. The ovarian tissues were shredded and digested with 2.0 ml of hyaluronidase (0.1%, Sigma-Aldrich, St Louis, MO, USA) for 1 minute at 37°C. The tissue suspension was gently pipetted,addedto 200 μlof fetal bovine serum (Gibco, Gaithersburg, MD, USA) to terminate the digestion, and then filtered through a 200-mesh cell sieve. The filtrate was added to 5.0 ml of PBS and mixed, then centrifuged at 1500 r/min for 5 min at 10°C. The supernatant was discarded, and the pellet was resuspended in 5.0 ml of PBS and centrifuged at 1500 r/min for 5 min at 10°C. The supernatant was discarded, and the cell pellet was resuspended in DMEM:F12 (1:1) medium containing 15% fetal bovine serum, 10 ng/ml basic fibroblast growth factor (bFGF), 10 ng/ml epidermal growth factor (EGF), 2 mM L-glutamine,

10 ng/ml growth hormone (Gh) and 15 ng/mlestradiol (E2) (all reagents were purchased from Gibco, Gaithersburg, MD, USA). Cells were seeded in 6-well-plates and incubated at 37°C with 5% CO_2 until 80% confluent. MOGCs were divided into two groups, with 3 parallel controls in each group. The cells in each POF group were treated with cyclophosphamide (IC_{50} concentration: 38.721 μM) for 24 hours. The PBS (control) group cells were incubated with an equal volume of PBS for 24 hours.

Hematoxylin-eosin staining

Briefly [3], all fresh tissue was soaked in 4% paraformaldehyde (Sigma-Aldrich, St. Louis, USA) for 30 minutes of fixation at room temperature, followed by ethanol gradient dehydration, paraffin embedment, sectioning (6 μm in thickness), and deparaffinization in xylene. Tissue sections were stained with haematoxylin-eosin (H & E, Sigma- Aldrich, St. Louis, USA), clarified in xylene (Sigma-Aldrich, St. Louis, USA) and mounted in neutral resin (Sigma-Aldrich, St. Louis, USA).

Western blot

Briefly [7], total protein from each group of samples was used for 12% SDS-PAGE (Bio-Rad Laboratories, Inc., California, USA); upon completion, the proteinwas transferred to a PVDF membrane (Millipore, Bedford, MA, USA). After blocking and washing the membrane, incubation with a primary antibody was carried out at 37°C for 45 min. After sufficiently washing the membrane, incubation with a secondary antibody was carried out at 37°C for 45 min. The membrane was washed 4 times, with 14 minutes per wash, with TBST (Bio-Rad Laboratories, Inc., California, USA) at room temperature. The membrane was then developed by ECL enhanced chemiluminescence (Bio-Rad Laboratories, Inc., California, USA) and exposed to Kodak XAR-5 films (Sigma-Aldrich Chemical).

Flow cytometry-PI staining analysis of the cell cycle

Briefly [8], 5×10^5/mlcells were collected and fixed in 1 ml of 70% ice-cold ethanol for 48 hours. After centrifugation at 1500 r/min for 5 min at 4°C, cell pellets were harvested and stained withPI staining solution (Sigma-Aldrich, St. Louis, USA) in the darkat 4°C for 30 min.

Flow cytometry (Quanta SC, Beckman Coulter INC) was then used to analyse the cell cycle distribution of each group of cells (a total of 20,000), and data analysis was conducted using CellQuest software.

Co-IP

Briefly [22], 1×10^8/ml cells were lysed using western and IP cell lysate (Beyotime Biotechnology). A total of 800 μl of total protein sample was taken, the protein concentration was adjusted to 1 mg/ml, and 1 μg of IgG and 20 μl of fully resuspended protein a agarose (Beyotime Biotechnology, HangZhou, China) were added to the samplesand shaken slowly at 4°C for 60 minutes, followed by centrifugation at 2500 r/min for 5 minutes. The centrifuged protein supernatant was collected, to which 1 μg of primary antibody was added,and the sample was then shaken slowly at 4°C for 12 hours, followed by the addition of another 20 μl of fully resuspended protein a agarose andshaking slowly at 4°C for 3 hours. After centrifugation at 2500 r/min for 5 minutes, the supernatant was discarded, and protein a agarose was washed with ice-cold PBS three times,with 15 minutes per wash. After centrifugation, protein a agarose was added to 100 μl of western and IP cell lysate (Beyotime Biotechnology, Hang Zhou, China), incubated in a 100°C water bath for 15 minutes and centrifuged at 12000 r/min for 10 minutes. The supernatant was collected and stored at -80°C.

RNA extraction and quantitative analysis

Total RNA was extracted from each group of cells according to theTRIzolmanual (Invitrogen). Subsequently, to each RNA sample, 10 U of DNase I (Sigma) was added,and the samples were incubated at 37°C for 30 min to remove residual DNA. The mRNA in the total RNA samples was isolated and purified using anOligotex mRNA Midi Kit (Qiagen). Quantification of the RNA concentration and integrity was determined using an Agilent 2100 Bioanalyzer and an Agilent RNA 6000 Nano Kit.

Establishment of cDNA sequencing libraries and high-throughput RNA-Seq

The following analysis was conducted by Shanghai FengHe InfoTech Ltd (Shanghai, China). According to their experimental proce-
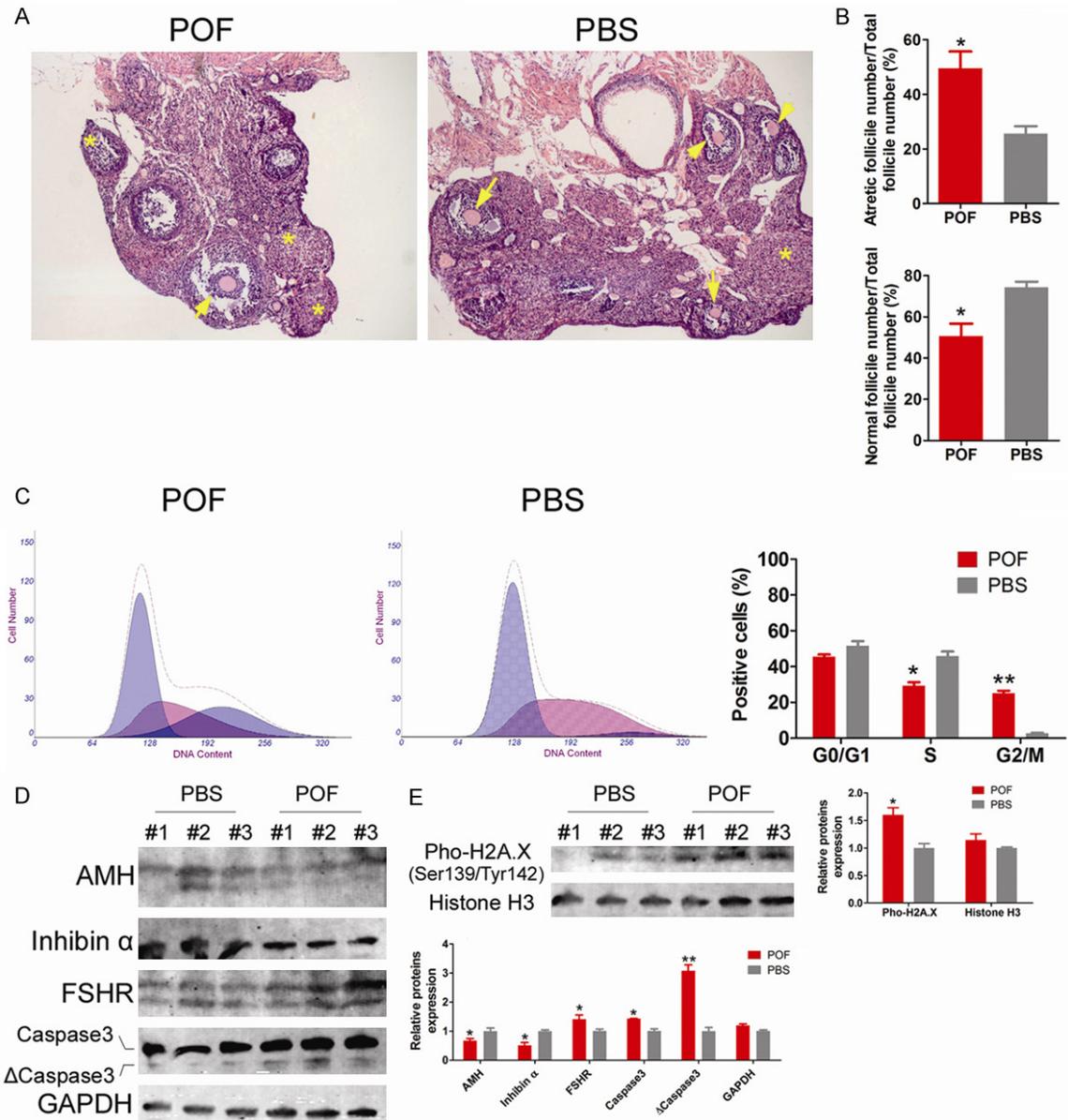
Figure 1. Cyclophosphamide significantly induced POFoccurrence and OGC damage and apoptosis. A. Histopathologic analysis of H & E staining showed that the POF group mice had severe ovarian atrophy, significantly increased atretic follicles (indicated by *), significantly reduced numbers of normal follicles in various stages (indicated by the black arrow), reduced ovarian volume, and dense interstitial area. Magnification is 200 ×. B. The proportion of ovarian atretic follicles in the POF group was significantly higher than that in the PBS group, and the proportion of normal follicles in the POF group was significantly lower than that in the PBS group. *P < 0.05 vs. PBS group, n = 3. C. Flow cytometry cell cycle analysis showed that the number of OGCs in the S phase of the cell cycle was significantly decreased in the POF group, while the number in the G2/M phase was significantly increased in the POF group. **P < 0.01 vs. PBS group, *P < 0.05 vs. PBS group, n = 3. D. Western blot results showed that the mOGCs of the POF group expressed significantly higher levels of activated Caspase 3 fragment (ΔCaspase 3) protein than did the mOGCs of the PBS group, while expressing significantly lower levels of AMH and Inhibin α proteins. **P < 0.01 vs. PBS group, *P < 0.05 vs. PBS group, n = 3. E. Western blot results showed that the mOGCs of the POF group expressed significantly higher levels of phosphorylated H2A.X (pho-H2A.X) protein than did the mOGCs of the PBS group, while expressing significantly lower levels of AMH and Inhibin α proteins. *P < 0.05 vs. PBS group, n = 3.

dures, a random fragment sequencing library was constructed using aSOLiD Whole Trans-criptome Analysis Kit (Life technologies). Nucleic acid cleaving reagents were added, and

the mRNA was randomly disrupted into short segments in a shaking incubator. First-strand cDNA was reverse transcribed using the fragmented mRNA as the template. Second-strand cDNA was synthesized using a second-strand DNAsynthesis reaction system consisting of DNA polymerase I, dNTPs and RNase H (Sigma). The synthesized DNA was purified using a DNA purification kit and recovered. Thebase 'A' was added to the 3' end of the cDNA, followed by ligation to the adapter, to complete the blunt end repair reaction. Subsequently, DNA fragment size selection was performed. Finally, the cDNA was used for PCR amplification to obtain a sequencing library. The constructed library was qualified using an Agilent 2100 Bioanalyzer and the ABI StepOnePlus Real-Time PCR System and was subjected to high-throughput sequencing using an Illumina HiSeq™ 2000 Sequencer after passing quality control.

Statistical analysis

Each experiment was performed as least three times, and data are shown as the mean ± SE where applicable, and differences were evaluated using Student's t-tests. P < 0.05 was considered significant.

Results

Cyclophosphamide significantly enhances OGC injury and apoptosis

Histopathological analysis of HE stained samples showed that ovarian tissues of mice in the POF group had severe atrophy, reduced volume, and dense interstitial areas (**Figure 1**). The proportion of atretic follicles out of the total number of follicles was significantly increased (49.51% ± 10.79%), while the proportion of normal follicles out of the total number of follicles was significantly decreased (50.49% ± 10.79%) (**Figure 1**). In contrast, many normal follicles (74.36% ± 4.72%) were found in the ovaries of mice in the PBS group (control group), whereas atretic follicles were rare (25.64% ± 4.72%) (**Figure 1**). In addition, the cell cycle analysis of OGCs by flow cytometry indicated that the number of S phase OGCs in the POF group was significantly decreased, while the number of OGCs in the G2/M phase was significantly increased. Due to the large number of cells arrested in the G2/M phase, the rate of cell cycle progression

declined (**Figure 1**). mOGCs of WT adult C57 mice were isolated in vitro and were also purified and cultured. ThemOGCin vitro injury model was prepared using cyclophosphamide (POF group). Western blot results showed that mOGCs in the POF group expressed significantly higher levels of activated Caspase 3 fragment (ΔCaspase 3) and phosphorylated H2A.X (pho-H2A.X) proteinsthan did mOGCs in the PBS group, suggesting that cells entered the aging and apoptosis stage (**Figure 1**). However, mOGCs in the POF group showed significantly lower expression of AMH and Inhibin B proteins than did mOGCs in the PBS group, indicating a decrease in cellular health quality (**Figure 1**). The results suggest that cyclophosphamide significantly promotesOGC injury and apoptosis.

Cyclophosphamide causes transcription changes and functional disruptions of multiple mOGCs genes

We first used chromatographic analysis to confirm that the RNA derived from each group of mOGCs had high purity (1.8 < OD260/OD280 < 2.0) and met the concentration requirementsfor RNA-Seq (**Figure 2**). Subsequently, RNA-Seq techniques were used to analyze the differences in mOGCtranscriptomes between POF and control (PBS) mice. After obtaining the RNA-Seq sequencing results, the raw data were statistically analyzed and calibrated. First, we removedreads for barcode sequences and adapter sequences; removedreads with > 5% N content; removed consecutive bases atthe 5' and 3' ends with quality less than 10; removed low quality reads (where the number of bases with quality < 20 was greater than 20% of read length); and removed reads less than 30 bases in length. Through the above processes, we obtained clean data from six samples, and follow-up statistical induction and in-depth data mining analysis were conducted using these clean reads. We first used TopHat software (v2.0.8) and aligned the clean reads to the mouse reference genome GRCm38 using the default parameters. We then used theStringtie tool (V1.2.2) and obtained the raw reads information of each mouse gene alignment according to mouse gene annotation information provided by Gencode. The Limmapackage method of the R language was used to screen for genes with significantly different expression between the sample and control. Finally, corrected RNA-
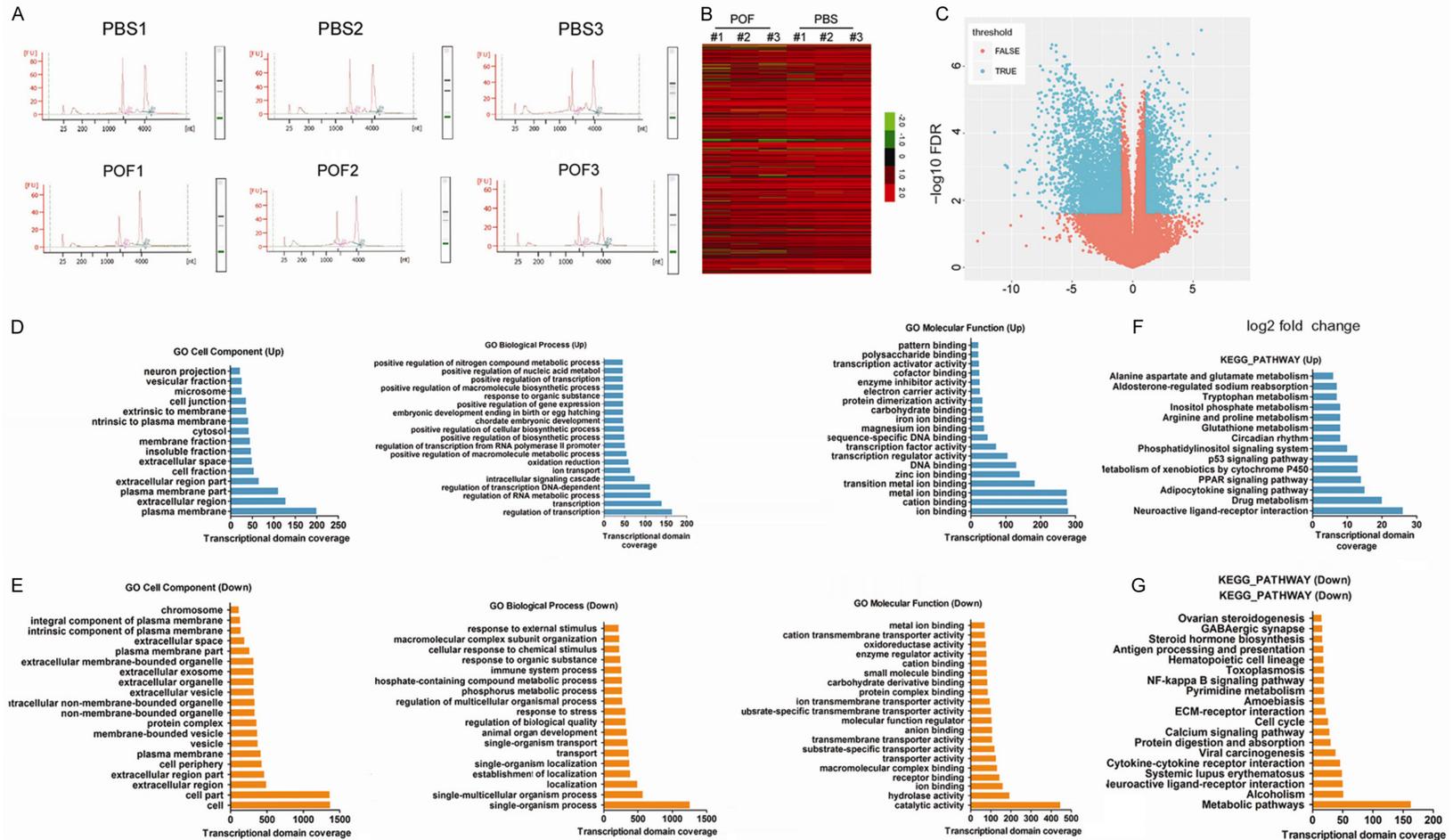
Figure 2. Cyclophosphamide led to transcription changes and functional disorders in multiple mOGC genes. A. Quantification of the purity and concentration of RNA of mOGCs from each group (1.8 < OD_{260}/OD_{280} < 2.0). B. RNA-Seq data are graphically displayed using the clustering index, with green representing genes with down-regulated transcription levels and red representing genes with up-regulated transcription levels. C. The relationship between differential analysis tests based on negative binomial distributions (P value, FPR) and differential transcripts. The differential transcript region in blue is the reliable region; the transcript region of the red portion is a non-feasible region. D. Results of Gene Ontology (GO) analysis of differential transcripts with up-regulated expression. E. Results of GO analysis of differential transcripts with down-regulated expression. F. Results of Kyoto Encyclopedia of Genes and Genomes (KEGG) enrichment analysis of differential transcripts with up-regulated expression. G. Results of KEGG enrichment analysis of differential transcripts with down-regulated expression.
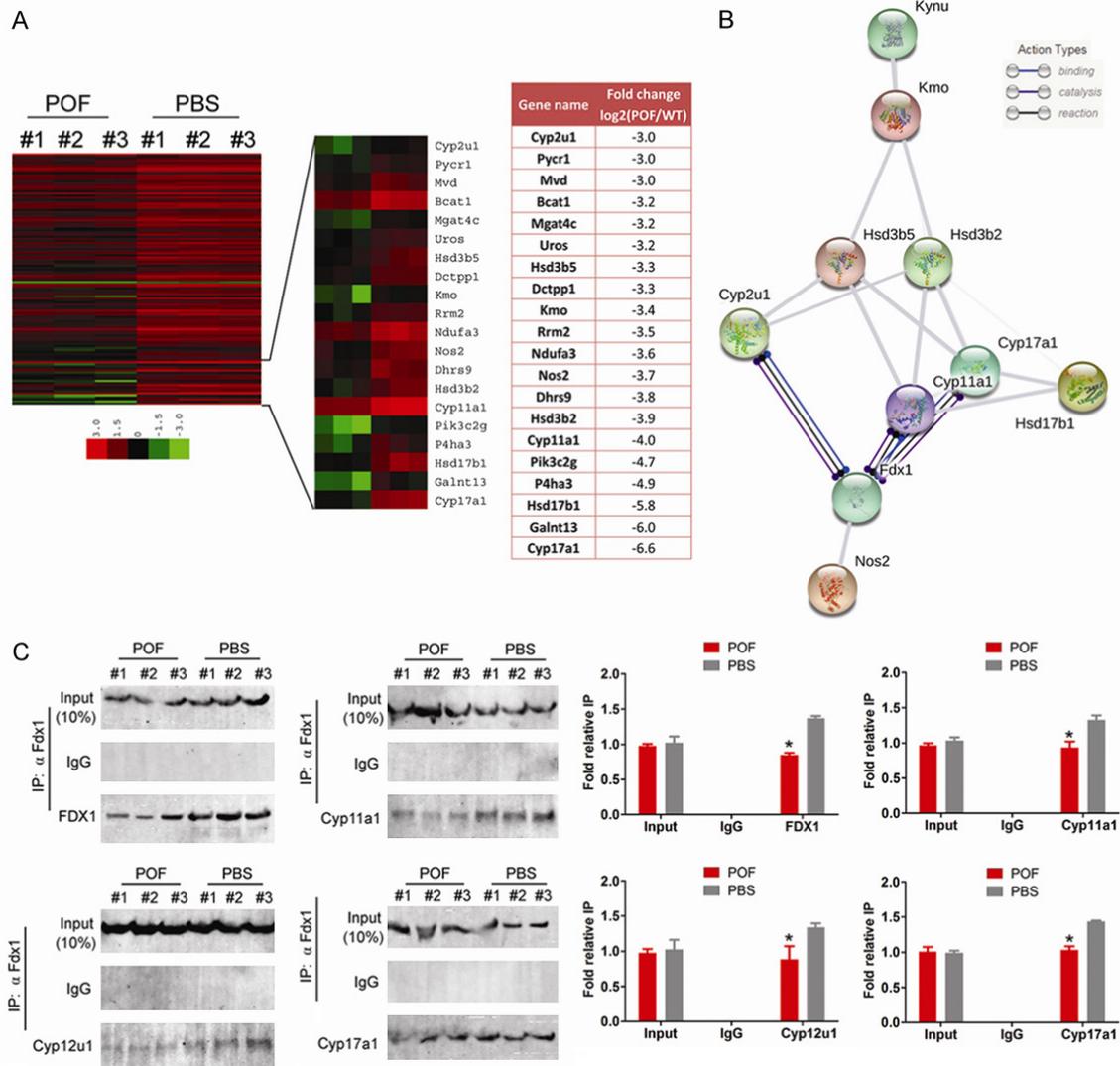
Figure 3. Cyclophosphamide down-regulated transcription activities of cytochrome P450 family genes involved in ovarian steroid metabolism in a targeted fashion in mOGCs. A. Clustered index results of differentially expressed genes involved in ovarian steroid genesis. KEGG pathway analysis identified a group of genes belonging to the functional group of ovarian steroid genesis, and its transcription activity was significantly lower in POF mOGCs than in the control group. Of the 122 genes, we screened 20 genes with log2 [POF/PBS] < -3.0. B. Prediction results using the String online tool for the differential transcripts suggest that there is interaction between the 10 proteins of the ovarian steroid genesis functional group. C. Co-IP western blot results show that the expression levels of Fdx1, Cyp2u1, Cyp12a1, and Cyp11a1 in the POF group are significantly lower than those in the PBS group, *P < 0.05 vs. PBS group, n = 3.

Seq results showed that there were 18,765 differentially transcribed genes between the two groups (**Figure 2**; Table S1), of which 192 were significantly up-regulated (log2 [POF/PBS] > 2.0) and 116 were significantly down-regulated (log2 [POF/PBS] < -4.0). Subsequently, differentially transcribed genes were subjected to Gene Ontology (GO) and Kyoto Encyclopedia of Genes and Genomes (KEGG) enrichment analysis using the DAVID online tool [23]. GO analysis suggested that transcription activities of genes related to the plasma membrane, extracellular region, cation binding, regulation of transcription, regulation of RNA metabolic process and ion binding functions were significantly increased in the POF group (**Figure 2**; Table S2), while transcription activities of genes related to the cell, cell parts, extracellular region, catalyt-

ic activity, single-organism process functions and single-multicellular organism process were significantly down-regulated (**Figure 2**; Table S2). KEGG analysis found that in the POF group, the transcription activities of genes belonging to the neuroactive ligand-receptor interaction and drug metabolism categories were significantly up-regulated, but genes belonging to the metabolic pathways category were significantly down-regulated (**Figure 2**; Table S3). The experimental results suggest that cyclophosphamide led to significanttranscription changes and functional disruptions in multiple mOGC genes.

Cyclophosphamide down-regulates the transcription activity of genes involved in mOGC ovarian steroid metabolism in a targeted fashion

Through KEGG pathway analysis, we identified a group of genes in POF mOGCs belonging to the ovarian steroidogenesis function withsignificantly reduced transcription activities compared to the control group (P < 0.01). Of the 122 genes, we screened 20 genes with log2 [POF/PBS] < -3.0 (**Figure 3**). Using the String V10.5 (https://string-db.org/) online analysis tool [24, 25], wepredicted whether there were some relationshipsamongthe proteins encoded by these genes. The results of the analysis showed that the protein products of 10 genes (Hynu, Kmo, Hsd3d5, Hsd3b2, Cyp2u1, Cyp12a1, Cyp11a1, Hsd17d1, Fdx1, and Nos2) interacted with each other (**Figure 3**). We also found that the Fdx1 protein is an important common node that can simultaneously interact with proteins such as Cyp2u1, Cyp12a1 and Cyp11a1 and bind, catalyse and activate their activities (**Figure 3**). To verify the above results, co-immunoprecipitation (IP)western blot was used to detect protein interactions. The experimental results showed that if theanti-Fdx1 antibody (α Fdx1 ab) was used for IP, then the expression signals for the remaining proteins such as Cyp2u1, Cyp12a1 and Cyp11a1 could be detected both in the POF group and in the PBS group (**Figure 3**). However, in the POF group, the expression levels of Fdx1, Cyp2u1, Cyp12a1, and Cyp11a1 were significantly lower than those in the PBS group (**Figure 3**). Our results reveal that cyclophosphamide significantly down-regulates the transcription activity of genes involved in the ovarian steroid metabolic function in a targeted fashion in mOGCs

as well as the expression level of protein-protein interaction networks.

Discussion

POF is a disease with serious consequences for the reproductive health of women [1, 2, 26]. The pathogenesis of POF is diverse, involving genetic abnormalities, induction by environmental toxins and chemotherapy drugs, immune system abnormalities, and endocrine disorders caused by mental stress [1, 2, 4, 26-28]. However, its exact cause is still unclear. In previous studies, we first established a model of cyclophosphamide-induced POF in mice and a model of immunosuppressant tripterygium glycosides-induced POF in rats [3, 4, 22]. The pathologic features of these two models, such as ovarian atrophy, apoptosis or necrosis of OGCs, increased atretic follicles, and severe decline in peripheral blood estrogen levels and significantly elevated FSH levels are consistent with human POF [1, 2]. This similarity suggests that the above two models are ideal and practical animal models to investigate drug-induced ovarian insufficiency. Although we have established animal models of POF, the mechanism of drug-induced POF has not yet been clearly established. In addition, genes with altered expression during the development of POF have not been clearly identified. OGCs play a very important role in oocyte maturation and ovarian function, as well as sex hormone release and endocrine maintenance, and our previous study has clarified that the apoptosis and necrosis of OGCs are important causes ofPOF [8, 22]. Therefore, in this study, we decided to use OGCs as the source material. We focused on the differential gene expression profiles in OGCs after cyclophosphamide treatment to obtain complete gene expression profile information as the basis for further study of biological effects. Therefore, we chose RNA-Seqas a means tostudy the gene transcription profile of OGCs. RNA-Seq uses high-throughput sequencing technology to analyse the sequences of cDNA derived from RNA reverse transcription and PCR amplification. With this technology, almost all transcripts in a specific organ or tissue of a particular species in a particular state can be obtained rapidly and comprehensively at the single-nucleotide level [10, 29, 30]. Compared with traditional subtractive hybridization, suppression subtractive hybridization,

and cDNA microarray, RNA-Seqhas the following advantages: compared with the traditional cDNA microarray hybridization screening technology, RNA-Seq does not need nucleic acid probes, and it is not necessary to know in advance the nucleic acid sequence of the gene to be sequenced. Therefore, RNA-Seq can use the sequencing method to conductfull transcriptome analysis of species with unknown genomesand to obtain differential information of gene transcripts. In addition, there are no issuesrelated to cross-reaction and background noise caused by the fluorescence analogue signal of traditional microarray hybridization, which greatly improves the resolution [10, 29, 30]. In addition, RNA-Seq has the obvious advantages of high throughput, low cost, and high sensitivity, and it enables us to obtain information about genes with low-expression levels [10, 29, 30]. We isolated OGCs from wild-type C57 mice and prepared the in vitro model of cyclophosphamide-induced apoptosis in OGCs. The RNA-Seq results showed that there were 18,765 differentially transcribed genes between the cyclophosphamide group and control group, of which 192 were significantly up-regulated and 116 were significantly down-regulated. In-depth analysis showed that the transcription activities of genes involved in the plasma membrane and extracellular region, regulation of transcription, RNA and drug metabolism and ion binding functions were significantly increased, while transcription activities of genes involved in the cells, catalytic activity, organism process and metabolic pathway functions were significantly down-regulated. Experimental data suggest that cyclophosphamide leads to significant transcription changes and functional disordersin multiple mOGCs genes.

In cells, cytochrome P450 is mainly distributed in the endoplasmic reticulum and the mitochondrial inner membrane, and it acts as a terminal oxygenase in the synthesis of steroid hormones in the body [20, 21]. Some studies have shown that cytochrome P450 is a key enzyme in the metabolism of drugs and has a significant impact on cytokines and thermoregulation [20, 21]. In the body, Cyp containing iron ions binds to drug molecules and accepts an electron delivered from NADPH-P450 reductase, which converts iron ions to divalent ferrous ions [20, 21]. Subsequently, it binds with one molecule of oxygen, one proton, and the

second electron to form the $Fe_2+OOH \cdot DH$ complex, which binds to another proton to produce water and iron oxide complex $(FeO)_3+ \cdot DH$ [20, 21]. $(FeO)_3+ \cdot DH$ extracts a hydrogen atom from $\cdot DH$ to form a pair of transient free radicals. The oxidized drug is released from the complex, and the P450 enzyme is regenerated [20, 21]. Dasari et al. found that mouse mitochondrial CYP1A1 is an outer membrane protein that exhibits high affinity for FDX1 and mediates the N-terminal demethylation of a wide range of tricyclic drugs such as anti-depressant drugs, analgesics, and anti-psychotic drugsby binding to FDXR [31]. This study confirms that thebinding ability between CYP1A1 and FDX1 is strong [31]. Roumaud et al. reported that in the mouse testicular stromal MA-10cells, the transcription factors SF1 and cJUNcould act together at a specific site of the Fdx1 promoter and activate its transcription [32]. Subsequently, the Fdx1 protein supports steroid biosynthesis in cells through electron transfer to the rate-limiting enzyme CYP11A1. CYP11A1 catalyses the conversion of cholesterol into pregnenolone in the mitochondria via sidechain cleavage [32]. The above study confirms that CYP1A1 and FDX1 are involved in steroid hormone synthesis [32]. In the present study, high-throughput RNA-Seq analysis showed that the transcription activities of the Cyp2u1, Cyp11a1, Cyp17a1 and Fdx1 genes were all significantly decreased after cyclophosphamide treatment of OGCs. Although the degree of decline was not the same, the trend was the same. In addition, coupled with the results of the protein-protein interaction network and several previous studies, we have reason to believe that the protein products of these four genes interact with each other. After cyclophosphamide treatment in mice, pathologic features of POF appeared randomly, and one of the most important phenomena was the significant decrease of AMH and E2 in OGCs, which marked the diminished ability of OGCs to synthesize hormones. It is likely that cyclophosphamide, by inhibiting the transcription activity of these four genes, eventually leads to a decrease in the ability of OGCs to synthesize and release hormones.

RNA-Seq high-throughput screening analysis demonstrated that the damage tomOGCsby cyclophosphamide was achieved through its impacts on multiple pathways and the transcription activities of multiple target genes.

Among them, the protein network consisting of the cytochrome P450 family membersFdx1, Cyp17a1, Cyp11a1, and Cyp2u1 is a new potential biomarker of OGC damage in POF in mice.

Acknowledgements

Disclosure of conflict of interest

None.

Address correspondence to: Dr. Te Liu, Department of Pathology, School of Medicine,Yale University, 10 Amistad St, New Haven, Connecticut 06520, USA. Tel: 1-203-7856047; Fax: 1-203-7852293; E-mail: te.liu@yale.edu; Dr. Ying Xiong, Department of Gynaecology and Obestetrics, Xinhua Hospital Affiliated to Shanghai Jiaotong University School of Medicine, 1665 Kongjiang Road, Shanghai 200092, China. Tel: 86-21-25078999; Fax: 86-21-25078999; E-mail: 2217060331@qq.com

References

[1] Beck-Peccoz P and Persani L. Premature ovarian failure. Orphanet J Rare Dis 2006; 1: 9.

[2] Vujovic S, Ivovic M, Tancic-Gajic M, Marina L, Barac M, Arizanovic Z, Nenezic A, Ivanisevic M, Micic J, Sajic S and Micic D. Premature ovarian failure. Srp Arh Celok Lek 2012; 140: 806-811.

[3] Liu T, Huang Y, Zhang J, Qin W, Chi H, Chen J, Yu Z and Chen C. Transplantation of human menstrual blood stem cells to treat premature ovarian failure in mouse model. Stem Cells Dev 2014; 23: 1548-1557.

[4] Liu T, Wang S, Li Q, Huang Y, Chen C and Zheng J. Telocytes as potential targets in a cyclophosphamide-induced animal model of premature ovarian failure. Mol Med Rep 2016; 14: 2415-2422.

[5] Liu TE, Wang S, Zhang L, Guo L, Yu Z, Chen C and Zheng J. Growth hormone treatment of premature ovarian failure in a mouse model via stimulation of the Notch-1 signaling pathway. Exp Ther Med 2016; 12: 215-221.

[6] Liu T, Huang Y, Guo L, Cheng W and Zou G. CD44+/CD105+ human amniotic fluid mesenchymal stem cells survive and proliferate in the ovary long-term in a mouse model of chemotherapy-induced premature ovarian failure. Int J Med Sci 2012; 9: 592-602.

[7] Liu T, Qin W, Huang Y, Zhao Y and Wang J. Induction of estrogen-sensitive epithelial cells derived from human-induced pluripotent stem cells to repair ovarian function in a chemotherapy-induced mouse model of premature ovarian failure. DNA Cell Biol 2013; 32: 685-698.

[8] Xiong Y, Liu T, Wang S, Chi H, Chen C and Zheng J. Cyclophosphamide promotes the proliferation inhibition of mouse ovarian granulosa cells and premature ovarian failure by activating the lncRNA-Meg3-p53-p66Shc pathway. Gene 2017; 596: 1-8.

[9] Chu Y and Corey DR. RNA sequencing: platform selection, experimental design, and data interpretation. Nucleic Acid Ther 2012; 22: 271-274.

[10] Wang Z, Gerstein M and Snyder M. RNA-Seq: a revolutionary tool for transcriptomics. Nat Rev Genet 2009; 10: 57-63.

[11] Maher CA, Kumar-Sinha C, Cao X, Kalyana-Sundaram S, Han B, Jing X, Sam L, Barrette T, Palanisamy N and Chinnaiyan AM. Transcriptome sequencing to detect gene fusions in cancer. Nature 2009; 458: 97-101.

[12] Ingolia NT, Brar GA, Rouskin S, McGeachy AM and Weissman JS. The ribosome profiling strategy for monitoring translation in vivo by deep sequencing of ribosome-protected mRNA fragments. Nat Protoc 2012; 7: 1534-1550.

[13] Kukurba KR and Montgomery SB. RNA Sequencing and analysis. Cold Spring Harb Protoc 2015; 2015: 951-969.

[14] Mootha VK, Bunkenborg J, Olsen JV, Hjerrild M, Wisniewski JR, Stahl E, Bolouri MS, Ray HN, Sihag S, Kamal M, Patterson N, Lander ES and Mann M. Integrated analysis of protein composition, tissue diversity, and gene regulation in mouse mitochondria. Cell 2003; 115: 629-640.

[15] Dickinson ME, Flenniken AM, Ji X, Teboul L, Wong MD, White JK, Meehan TF, Weninger WJ, Westerberg H, Adissu H, Baker CN, Bower L, Brown JM, Caddle LB, Chiani F, Clary D, Cleak J, Daly MJ, Denegre JM, Doe B, Dolan ME, Edie SM, Fuchs H, Gailus-Durner V, Galli A, Gambadoro A, Gallegos J, Guo S, Horner NR, Hsu CW, Johnson SJ, Kalaga S, Keith LC, Lanoue L, Lawson TN, Lek M, Mark M, Marschall S, Mason J, McElwee ML, Newbigging S, Nutter LM, Peterson KA, Ramirez-Solis R, Rowland DJ, Ryder E, Samocha KE, Seavitt JR, Selloum M, Szoke-Kovacs Z, Tamura M, Trainor AG, Tudose I, Wakana S, Warren J, Wendling O, West DB, Wong L, Yoshiki A; International Mouse Phenotyping Consortium; Jackson Laboratory; Infra-

structure Nationale PHENOMIN, Institut Clinique de la Souris (ICS); Charles River Laboratories; MRC Harwell; Toronto Centre for Phenogenomics; Wellcome Trust Sanger Institute; RIKEN BioResource Center, MacArthur DG, Tocchini-Valentini GP, Gao X, Flicek P, Bradley A, Skarnes WC, Justice MJ, Parkinson HE, Moore M, Wells S, Braun RE, Svenson KL, de Angelis MH, Herault Y, Mohun T, Mallon AM, Henkelman RM, Brown SD, Adams DJ, Lloyd KC, McKerlie C, Beaudet AL, Bucan M and Murray SA. High-throughput discovery of novel developmental phenotypes. Nature 2016; 537: 508-514.

[16] Pagliarini DJ, Calvo SE, Chang B, Sheth SA, Vafai SB, Ong SE, Walford GA, Sugiana C, Boneh A, Chen WK, Hill DE, Vidal M, Evans JG, Thorburn DR, Carr SA and Mootha VK. A mitochondrial protein compendium elucidates complex I disease biology. Cell 2008; 134: 112-123.

[17] Hansen J, Floss T, Van Sloun P, Fuchtbauer EM, Vauti F, Arnold HH, Schnutgen F, Wurst W, von Melchner H and Ruiz P. A large-scale, gene-driven mutagenesis approach for the functional analysis of the mouse genome. Proc Natl Acad Sci U S A 2003; 100: 9918-9922.

[18] Skarnes WC, Rosen B, West AP, Koutsourakis M, Bushell W, Iyer V, Mujica AO, Thomas M, Harrow J, Cox T, Jackson D, Severin J, Biggs P, Fu J, Nefedov M, de Jong PJ, Stewart AF and Bradley A. A conditional knockout resource for the genome-wide study of mouse gene function. Nature 2011; 474: 337-342.

[19] Diez-Roux G, Banfi S, Sultan M, Geffers L, Anand S, Rozado D, Magen A, Canidio E, Pagani M, Peluso I, Lin-Marq N, Koch M, Bilio M, Cantiello I, Verde R, De Masi C, Bianchi SA, Cicchini J, Perroud E, Mehmeti S, Dagand E, Schrinner S, Nurnberger A, Schmidt K, Metz K, Zwingmann C, Brieske N, Springer C, Hernandez AM, Herzog S, Grabbe F, Sieverding C, Fischer B, Schrader K, Brockmeyer M, Dettmer S, Helbig C, Alunni V, Battaini MA, Mura C, Henrichsen CN, Garcia-Lopez R, Echevarria D, Puelles E, Garcia-Calero E, Kruse S, Uhr M, Kauck C, Feng G, Milyaev N, Ong CK, Kumar L, Lam M, Semple CA, Gyenesei A, Mundlos S, Radelof U, Lehrach H, Sarmientos P, Reymond A, Davidson DR, Dolle P, Antonarakis SE, Yaspo ML, Martinez S, Baldock RA, Eichele G and Ballabio A. A high-resolution anatomical atlas of the transcriptome in the mouse embryo. PLoS Biol 2011; 9: e1000582.

[20] Choudhary D, Jansson I, Stoilov I, Sarfarazi M and Schenkman JB. Expression patterns of mouse and human CYP orthologs (families 1-4) during development and in different adult tissues. Arch Biochem Biophys 2005; 436: 50-61.

[21] Meunier B, de Visser SP and Shaik S. Mechanism of oxidation reactions catalyzed by cytochrome p450 enzymes. Chem Rev 2004; 104: 3947-3980.

[22] Liu TE, Zhang L, Wang S, Chen C and Zheng J. Tripterygium glycosides induce premature ovarian failure in rats by promoting p53 phosphorylation and activating the serine/threonine kinase 11-p53-p21 signaling pathway. Exp Ther Med 2015; 10: 12-18.

[23] Dennis G Jr, Sherman BT, Hosack DA, Yang J, Gao W, Lane HC and Lempicki RA. David: database for annotation, visualization, and integrated discovery. Genome Biol 2003; 4: P3.

[24] Franceschini A, Szklarczyk D, Frankild S, Kuhn M, Simonovic M, Roth A, Lin J, Minguez P, Bork P, von Mering C and Jensen LJ. STRING v9.1: protein-protein interaction networks, with increased coverage and integration. Nucleic Acids Res 2013; 41: D808-815.

[25] Shannon P, Markiel A, Ozier O, Baliga NS, Wang JT, Ramage D, Amin N, Schwikowski B and Ideker T. Cytoscape: a software environment for integrated models of biomolecular interaction networks. Genome Res 2003; 13: 2498-2504.

[26] Correction to: Cytogenetic analysis of 179 Iranian women with premature ovarian failure. Gynecol Endocrinol 2013; 29: 727.

[27] Bandyopadhyay S, Chakrabarti J, Banerjee S, Pal AK, Goswami SK, Chakravarty BN and Kabir SN. Galactose toxicity in the rat as a model for premature ovarian failure: an experimental approach readdressed. Hum Reprod 2003; 18: 2031-2038.

[28] Qin Y, Sun M, You L, Wei D, Sun J, Liang X, Zhang B, Jiang H, Xu J and Chen ZJ. ESR1, HK3 and BRSK1 gene variants are associated with both age at natural menopause and premature ovarian failure. Orphanet J Rare Dis 2012; 7: 5.

[29] Tariq MA, Kim HJ, Jejelowo O and Pourmand N. Whole-transcriptome RNAseq analysis from minute amount of total RNA. Nucleic Acids Res 2011; 39: e120.

[30] Richard H, Schulz MH, Sultan M, Nurnberger A, Schrinner S, Balzereit D, Dagand E, Rasche A, Lehrach H, Vingron M, Haas SA and Yaspo ML. Prediction of alternative isoforms from exon expression levels in RNA-Seq experiments. Nucleic Acids Res 2010; 38: e112.

[31] Dasari VR, Anandatheerthavarada HK, Robin MA, Boopathi E, Biswas G, Fang JK, Nebert DW and Avadhani NG. Role of protein kinase C-mediated protein phosphorylation in mitochondrial translocation of mouse CYP1A1, which contains a non-canonical targeting signal. J Biol Chem 2006; 281: 30834-30847.

[32] Roumaud P, Rwigemera A and Martin LJ. Transcription factors SF1 and cJUN cooperate to activate the Fdx1 promoter in MA-10 Leydig cells. J Steroid Biochem Mol Biol 2017; 171: 121-132.

Biomarkers of mice POF determined by RNA-Seq

Table S1. Different transcription genes of POF group and control group

GENE_ID	POF			PBS			Fold change (log2 [POF group/ PBS group])	Gene_Functions
	#1	#2	#3	#1	#2	#3		
Serpina3m	1913.670	3229.330	2514.670	9.333	63.667	94.333	5.516	Serine (or cysteine) peptidase inhibitor, clade A, member 3M
Tat	421.333	396.000	66.667	4.333	5.333	10.667	5.442	tyrosine aminotransferase
Cyp2e1	54781.500	45280.000	49910.500	285.500	2107.500	1528.000	5.257	Cytochrome P450, family 2, subfamily e, polypeptide 1
Slc5a11	906.375	866.625	682.125	9.000	6.625	60.125	5.018	Solute carrier family 5 (sodium/glucose cotransporter), member 11
Serpina3n	32805.500	27184.000	29822.500	807.000	1112.500	949.000	4.969	Serine (or cysteine) peptidase inhibitor, clade A, member 3N
Mc5r	98.000	9.000	86.000	2.000	2.000	4.000	4.592	Melanocortin 5 receptor
Serpina3k	794.000	1743.000	592.500	9.000	57.000	64.000	4.589	Serine (or cysteine) peptidase inhibitor, clade A, member 3K
Obp2a	392.500	346.000	528.000	42.500	9.000	2.000	4.565	Odorant binding protein 2A
Gm12259	133.000	8.500	11.000	3.000	1.500	2.500	4.445	Predicted gene 12259
Tnn	587.333	254.000	299.333	7.333	26.667	20.000	4.401	Tenascin N
Kcnj16	55.000	247.857	7.857	6.429	2.143	6.286	4.386	Potassium inwardly-rectifying channel, subfamily J, member 16
Itih4	1645.000	1412.330	1559.670	77.500	70.333	84.667	4.312	Inter-alpha-trypsin inhibitor heavy chain family, member 4
Hao1	49.667	105.333	56.000	3.000	1.000	6.667	4.306	Hydroxyacid oxidase 1, liver
Gm26813	341.000	130.000	153.000	4.000	14.000	16.000	4.198	Predicted gene 26813
Apoc4	270.000	480.000	377.000	2.500	24.500	38.500	4.105	Apolipoprotein C-IV
Gm16217	37.000	41.500	5.000	1.000	2.000	2.000	4.062	Predicted gene 16217
Ftcd	60.500	93.750	75.750	7.250	1.250	5.750	4.013	Formiminotransferase cyclodeaminase
Gm12630	81.000	78.000	71.000	6.000	4.000	5.000	3.939	Predicted gene 12630
Serpina3i	1171.000	1261.000	899.000	49.000	77.333	91.000	3.938	Serine (or cysteine) peptidase inhibitor, clade A, member 3I
Cyp2w1	3.000	223.500	12.000	8.000	2.000	6.000	3.898	Cytochrome P450, family 2, subfamily W, polypeptide 1
Gm11033	4.250	0.500	16.250	0.250	0.750	0.500	3.807	Predicted gene 11033
Cidec	14839.400	11224.400	12141.000	175.600	1355.600	1261.400	3.774	Cell death-inducing DFFA-like effector c
Lta	73.500	6.000	2.000	1.500	2.000	3.000	3.648	Lymphotoxin A
Mboat4	81.500	47.500	99.000	6.000	8.000	5.000	3.585	Membrane bound O-acyltransferase domain containing 4
Serpina3b	563.500	571.000	515.000	41.500	56.000	40.500	3.579	Serine (or cysteine) peptidase inhibitor, clade A, member 3B
Pla2g10	730.600	198.400	461.600	34.600	34.600	47.400	3.576	Phospholipase A2, group X
Cfd	75731.500	58491.000	69723.000	1982.000	9118.500	6347.000	3.547	Complement factor D (adipsin)
Gm10800	142.000	50.500	430.000	10.500	33.000	10.000	3.540	Predicted gene 10800
Gm18294	19.500	1.000	171.000	3.000	11.500	2.000	3.537	Predicted gene 18294
Cdkn1a	15145.200	11233.000	14422.500	1240.250	1368.000	1063.750	3.474	Cyclin-dependent kinase inhibitor 1A (P21)
Gdf15	720.667	825.333	808.333	45.000	88.000	80.000	3.466	Growth differentiation factor 15
Gm14016	10.000	86.000	99.000	1.000	6.000	11.000	3.437	Predicted gene 14016
Gm6537	115.000	89.500	149.000	1.000	14.500	17.500	3.421	Predicted gene 6537
Slc10a6	2664.000	2129.500	2192.500	173.000	226.000	258.500	3.409	Solute carrier family 10 (sodium/bile acid cotransporter family), member 6
Aldh3b2	814.500	253.000	662.000	69.000	71.500	25.500	3.381	Aldehyde dehydrogenase 3 family, member B2
Tigit	202.000	225.500	803.500	34.500	43.000	45.500	3.323	T cell immunoreceptor with Ig and ITIM domains
Rpph1	2.000	9.000	89.000	3.000	2.000	5.000	3.322	Ribonuclease P RNA component H1

1

Biomarkers of mice POF determined by RNA-Seq

Apod	2519.290	2860.430	3167.860	214.571	411.857	241.571	3.300	Apolipoprotein D
Kcnc4	305.500	178.000	252.500	2.000	24.000	51.000	3.257	Potassium voltage gated channel, Shaw-related subfamily, member 4
Inmt	3099.670	2899.670	2518.000	259.333	328.333	310.333	3.246	Indolethylamine N-methyltransferase
Cyp1a1	540.000	110.000	556.000	48.000	69.000	16.000	3.181	Cytochrome P450, family 1, subfamily a, polypeptide 1
Marco	534.000	208.000	5.333	40.333	9.333	33.667	3.165	Macrophage receptor with collagenous structure
Pon1	246.200	47.200	166.600	3.800	15.400	32.200	3.162	Paraoxonase 1
Gm13369	99.000	56.000	158.000	10.000	8.000	17.000	3.161	Predicted gene 13369
Pck1	4601.200	2828.000	4463.000	473.400	412.600	449.800	3.154	Phosphoenolpyruvate carboxykinase 1 (soluble)
Hp	30638.500	25718.000	26418.500	1150.000	5224.500	2940.500	3.152	Haptoglobin
Irf4	4809.330	3196.670	2956.670	840.000	198.000	243.333	3.097	Interferon regulatory factor 4
Acsm3	2355.890	1974.000	1772.000	184.667	288.778	243.111	3.090	Acyl-CoA synthetase medium-chain family member 3
Gm13055	85.500	102.000	122.500	2.000	14.500	20.000	3.086	Predicted gene 13055
Gm5607	123.000	83.667	161.333	3.000	19.000	21.667	3.075	Predicted gene 5607
Clcn1	5.727	162.545	66.455	2.364	15.273	10.636	3.053	chloride channel, voltage-sensitive 1
Rtn4rl2	408.500	276.250	475.250	24.000	71.500	44.250	3.053	reticulon 4 receptor-like 2
Slc36a2	4295.670	2884.330	4372.330	152.000	683.667	569.000	3.040	solute carrier family 36 (proton/amino acid symporter), member 2
Per1	30163.400	24862.700	35298.700	3699.000	3456.290	4039.860	3.012	period circadian clock 1
Myt1l	1.000	17.667	100.667	3.667	3.333	8.333	2.960	myelin transcription factor 1-like
Psapl1	91.000	36.000	5.000	7.000	4.000	6.000	2.957	prosaposin-like 1
Gm12840	271.500	193.000	456.500	9.500	62.000	49.000	2.934	Predicted gene 12840
Gm20389	1.000	192.000	9.500	4.000	8.500	14.000	2.934	Predicted gene 20389
Aspg	4020.500	2605.000	5314.000	960.500	214.000	397.000	2.926	asparaginase
Apol8	73.333	2.333	101.000	11.667	7.000	4.667	2.921	Apolipoprotein L 8
Slc22a28	5.000	0.500	94.500	1.000	6.000	6.500	2.889	solute carrier family 22, member 28
Olfr543	111.000	21.000	28.000	9.000	7.000	6.000	2.862	Olfactory receptor 543
Celf5	376.000	561.000	316.222	25.778	70.667	76.778	2.855	CUGBP, Elav-like family member 5
Gm15723	318.500	247.500	244.000	35.000	20.000	61.000	2.804	Predicted gene 15723
AU019990	122.750	24.000	174.500	10.500	17.000	18.750	2.796	Expressed sequence AU019990
Gm13346	30.000	43.000	72.000	8.000	11.000	2.000	2.788	Predicted gene 13346
Acr	356.000	211.000	345.000	25.000	52.500	57.000	2.761	acrosin prepropeptide
Cwh43	1753.000	1263.800	2235.000	140.600	347.000	287.000	2.761	cell wall biogenesis 43 C-terminal homolog
Slc22a2	157.000	38.500	78.500	8.000	24.500	8.500	2.740	solute carrier family 22 (organic cation transporter), member 2
Klb	579.000	901.000	490.000	37.500	148.000	112.000	2.727	Klotho beta
Fmo2	7514.170	5603.000	8099.330	742.333	929.000	1584.170	2.704	flavin containing monooxygenase 2
Gm16105	61.500	82.000	136.000	17.500	11.000	14.500	2.700	Predicted gene16105
Klf15	8359.670	7637.000	9138.000	853.333	1588.330	1494.000	2.675	Kruppel-like factor 15
Ccdc110	63.333	115.667	41.333	3.667	9.667	21.333	2.668	coiled-coil domain containing 110
Ces1c	327.500	179.000	397.000	23.750	49.000	70.750	2.654	Carboxylesterase 1C
Gm14027	1506.500	940.500	1112.500	105.500	264.500	199.000	2.645	Predicted gene 14027
Gm10086	2.000	137.000	59.000	12.000	13.000	7.000	2.629	Predicted gene 10086
Oprl1	186.500	184.500	68.833	11.000	31.500	28.667	2.628	opioid receptor-like 1

Biomarkers of mice POF determined by RNA-Seq

Gene							Value	Description
Gm9992	1925.500	1158.000	1633.500	185.000	329.500	250.000	2.625	Predicted gene 9992
Cyp3a57	229.667	159.000	128.000	47.000	16.667	20.333	2.621	Cytochrome P450, family 3, subfamily a, polypeptide 57
Gm26384	285.000	749.000	589.000	127.000	75.000	64.000	2.609	Predicted gene 26384
Klrb1-ps1	81.500	85.000	108.500	10.500	14.500	20.500	2.595	Killer cell lectin-like receptor subfamily B member 1, pseudogene 1
Serpina3h	368.000	228.667	556.000	19.667	102.000	73.667	2.561	Serine (or cysteine) peptidase inhibitor, clade A, member 3H
Pou3f3os	0.154	0.308	4.077	0.154	0.308	0.308	2.561	POU domain, class 3, transcription factor 3 adjacent noncoding transcript 1
Gm15727	176.000	78.000	220.000	20.000	32.000	29.000	2.549	Predicted gene 15727
Apoc1	3352.670	2478.000	3264.670	181.000	857.333	517.333	2.548	apolipoprotein C-I
Kcnj15	129.000	178.214	237.643	42.500	23.429	27.857	2.538	potassium inwardly-rectifying channel, subfamily J, member 15
RP23-329D23.4	132.333	59.667	24.000	6.333	15.667	15.333	2.532	RIKEN cDNA 2010310C07 gene
Olfr920	470.500	187.000	426.000	39.000	72.500	77.000	2.523	Olfactory receptor 920
Adamdec1	808.000	134.000	327.000	76.000	80.500	64.500	2.522	ADAM-like, decysin 1
Fam209	153.000	52.000	93.000	6.500	28.000	18.000	2.505	family with sequence similarity 209
Unc93a	1119.000	517.500	707.000	104.000	146.000	168.500	2.485	unc-93 homolog A (C. elegans)
Eda2r	2654.800	2268.600	2504.200	206.800	411.200	713.800	2.480	ectodysplasin A2 receptor
Mc2r	115.500	340.000	359.500	50.000	62.500	34.500	2.471	melanocortin 2 receptor
Luzp2	478.500	326.500	553.500	81.000	105.000	60.500	2.462	leucine zipper protein 2
Ucp3	70.400	340.000	131.400	6.600	37.600	54.200	2.461	uncoupling protein 3 (mitochondrial, proton carrier)
Gsta3	4024.000	4050.600	3724.000	572.200	801.200	769.600	2.461	glutathione S-transferase, alpha 3
Cyp2d37-ps	196.500	277.000	127.000	38.500	25.500	46.000	2.449	Cytochrome P450, family 2, subfamily d, polypeptide 37, pseudogene
Npc1l1	160.500	92.000	189.000	13.000	37.000	31.000	2.446	NPC1 like intracellular cholesterol transporter 1
Rgs1	724.700	661.200	831.700	84.800	121.400	200.800	2.446	regulator of G-protein signaling 1
Hsd11b1	1329.290	1347.140	1402.430	191.571	331.857	226.571	2.443	hydroxysteroid 11-beta dehydrogenase 1
Tktl1	271.000	68.667	320.333	24.667	51.333	47.333	2.420	transketolase-like 1
Gm13062	53.500	73.000	163.500	6.000	23.500	25.000	2.412	Predicted gene13062
Azgp1	141.500	86.000	6.000	13.000	5.000	26.000	2.408	alpha-2-glycoprotein 1, zinc
Gm20658	59.333	66.333	100.333	13.000	11.333	18.667	2.394	Predicted gene20658
Gm17281	96.000	85.500	165.000	11.000	38.500	16.500	2.392	Predicted gene17281
Ankdd1a	13.500	39.500	9.500	1.000	2.000	9.000	2.381	ankyrin repeat and death domain containing 1A
Umod	6.000	8.000	38.000	5.000	4.000	1.000	2.379	Uromodulin
Ccdc63	1.500	0.833	31.333	2.667	1.667	2.167	2.373	coiled-coil domain containing 63
RP24-497L5.5	450.000	222.000	716.500	54.500	91.000	123.500	2.368	predicted gene 8597
Elfn2	42.000	31.000	267.000	22.000	14.000	30.000	2.365	Leucine rich repeat and fibronectin type III, extracellular 2
Gm15338	129.000	142.000	35.500	2.000	39.500	18.000	2.365	Predicted gene 15338
Foxd3	1.000	5.000	97.000	14.000	4.000	2.000	2.365	Forkhead box D3
Gm12081	5.500	29.500	1.000	1.000	1.500	4.500	2.363	Predicted gene 12081
Hlf	3471.710	3145.860	4459.430	490.286	705.857	964.286	2.358	hepatic leukemia factor
Folh1	212.000	661.333	310.000	12.000	114.000	105.333	2.355	folate hydrolase 1
Nt5c1b	61.400	160.000	33.200	7.800	32.200	10.400	2.337	5'-nucleotidase, cytosolic IB
Gm11947	49.000	37.500	24.000	10.500	7.500	4.000	2.328	Predicted gene 11947
Ldhc	141.000	32.500	22.000	3.750	25.500	9.750	2.326	lactate dehydrogenase C

3

Biomarkers of mice POF determined by RNA-Seq

Psors1c2	72.000	54.000	197.000	2.000	17.000	47.000	2.291	psoriasis susceptibility 1 candidate 2
Trhde	377.250	311.750	823.000	122.500	68.000	118.500	2.291	TRH-degrading enzyme
Klf9	25569.500	18182.500	26879.500	3990.500	5599.500	4871.500	2.288	Kruppel-like factor 9
Hrct1	424.000	389.000	805.000	56.000	181.000	96.000	2.281	histidine rich carboxyl terminus 1
Cyp2d34	188.000	261.000	172.000	50.000	23.000	55.000	2.278	cytochrome P450, family 2, subfamily d, polypeptide 34
RP24-286D13.6	1191.000	962.500	961.500	82.000	356.500	208.000	2.269	predicted gene 29371
Ppp1r1c	1.667	23.167	1.667	0.667	4.500	0.333	2.268	protein phosphatase 1, regulatory (inhibitor) subunit 1C
Gm26583	151.500	222.000	23.000	10.000	46.500	26.000	2.265	Predicted gene 26583
Slc7a15	5446.000	4518.000	5990.250	594.000	1459.250	1283.750	2.257	solute carrier family 7 (cationic amino acid transporter, y+ system), member 15
RP24-285E3.4	53.500	144.000	181.000	19.000	24.000	36.500	2.251	predicted gene 28802
Ano2	448.571	27.143	67.000	18.714	40.714	54.714	2.249	anoctamin 2
Gm5639	50.000	10.000	6.000	3.000	9.000	2.000	2.237	Predicted gene 5639
Pnpla2	33383.000	31200.000	34990.200	7274.000	7550.120	6327.500	2.235	patatin-like phospholipase domain containing 2
Fmo3	41.000	128.000	61.667	21.000	16.667	11.333	2.235	flavin containing monooxygenase 3
Gabrq	260.667	146.000	32.333	18.667	48.667	26.667	2.223	gamma-aminobutyric acid (GABA) A receptor, subunit theta
Ces1d	10584.000	7744.400	10296.000	1452.200	2287.200	2389.800	2.223	carboxylesterase 1D
Dusp26	671.000	410.667	549.167	134.167	114.667	100.667	2.222	dual specificity phosphatase 26 (putative)
Wnt11	3740.670	3346.330	4564.500	259.000	989.333	1254.330	2.219	wingless-type MMTV integration site family, member 11
Asic3	204.500	155.000	293.500	48.000	39.000	53.500	2.217	acid-sensing (proton-gated) ion channel 3
Uchl1os	42.667	2.000	3.333	2.000	7.000	1.333	2.216	Uchl1 opposite strand transcript (head to head)
mt-Tk	26.000	19.000	61.000	6.000	12.000	5.000	2.204	tRNA lysine, mitochondrial
Acsl1	7237.110	5426.000	6493.670	788.444	1557.780	1826.890	2.199	acyl-CoA synthetase long-chain family member 1
Fcna	1073.330	1173.670	400.333	274.333	238.000	66.333	2.194	Ficolin A
Adig	826.250	797.250	1390.250	49.250	397.500	216.250	2.184	Adipogenin
Gm3510	95.000	2.000	28.000	11.000	8.500	8.000	2.184	Predicted gene3510
Dmrt2	154.500	234.500	324.000	10.000	90.000	57.000	2.183	doublesex and mab-3 related transcription factor 2
Sstr4	134.000	49.000	111.000	18.000	34.000	13.000	2.177	somatostatin receptor 4
Cyp2d10	223.000	263.000	172.000	58.000	35.000	53.000	2.172	Cytochrome P450, family 2, subfamily d, polypeptide 10
Gm15179	64.667	104.667	96.333	16.333	31.000	11.667	2.171	Predicted gene15179
Rpl18a-ps1	1.000	67.000	4.000	3.000	1.000	12.000	2.170	ribosomal protein L18A, pseudogene 1
Gm9522	372.000	311.000	292.000	45.000	105.000	67.000	2.168	Predicted gene9522
Gnmt	141.000	155.667	255.333	44.000	42.000	37.667	2.158	glycine N-methyltransferase
Mgat5b	107.800	16.600	22.800	22.800	4.000	6.200	2.157	mannoside acetylglucosaminyltransferase 5, isoenzyme B
Ascl2	96.000	220.000	249.000	23.000	67.667	36.000	2.157	achaete-scute family bHLH transcription factor 2
Gys2	21.333	47.667	74.333	1.333	24.000	7.000	2.148	glycogen synthase 2
Gm9286	48.000	29.000	5.000	6.000	9.500	3.000	2.148	Predicted gene9286
Plk5	870.200	728.600	635.400	12.800	249.200	242.200	2.148	polo like kinase 5
Cabp4	191.000	159.000	132.500	21.500	46.000	41.500	2.146	calcium binding protein 4
Gm12505	39.000	53.000	56.000	11.000	18.000	4.500	2.143	Predicted gene12505
Amy2a3	75.000	93.000	190.000	10.000	39.500	32.000	2.135	Amylase 2a3
Cebpd	5447.000	4321.000	6069.000	1811.000	843.000	966.000	2.129	CCAAT/enhancer binding protein (C/EBP), delta

Biomarkers of mice POF determined by RNA-Seq

Gm5466	228.000	270.000	261.000	28.000	92.000	54.000	2.125	Predicted gene5466
Amy2b	75.000	93.000	185.000	10.000	39.000	32.000	2.124	Amylase 2b
Isl2	86.167	0.833	7.667	7.333	4.667	9.833	2.116	insulin related protein 2
Amy2a4	75.000	93.000	185.000	10.000	39.500	32.000	2.115	Amylase 2a4
Rnf125	1321.500	848.000	1518.500	282.500	179.000	390.000	2.115	ring finger protein 125
Gm26805	27.500	55.500	29.500	8.500	7.000	10.500	2.113	Predicted gene26805
Arr3	49.375	2.375	15.750	4.750	7.375	3.500	2.111	arrestin 3, retinal
Amy2a2	75.000	93.000	184.000	10.000	39.500	32.000	2.111	amylase 2a2
BC051142	233.400	137.900	351.100	18.700	83.800	64.800	2.110	CDNA sequence BC051142
Mmp7	780.000	779.000	684.000	284.000	196.500	40.500	2.106	matrix metallopeptidase 7
Zbtb16	4929.500	4247.000	5455.500	968.000	1365.500	1077.000	2.101	zinc finger and BTB domain containing 16
DXBay18	67.000	15.000	27.000	6.000	14.000	5.500	2.096	DNA segment, Chr X, Baylor 18
Cldn8	696.000	344.000	1016.000	124.000	140.000	219.000	2.090	Claudin 8
Gm16998	139.000	20.500	106.500	14.000	18.500	30.000	2.089	Predicted gene16998
Igkv9-120	125.000	954.000	19.000	188.000	15.000	55.000	2.089	immunoglobulin kappa chain variable 9-120
Gm5406	457.000	168.000	302.000	6.000	113.000	100.000	2.082	Predicted gene5406
Plin4	17012.700	10618.700	15017.700	1774.670	3687.000	4629.670	2.079	Perilipin 4
Zc3h6	5807.330	4864.670	4864.000	781.000	1529.670	1378.000	2.074	zinc finger CCCH type containing 6
Adipoq	6197.670	6532.000	5696.670	297.000	2368.000	1722.330	2.070	adiponectin, C1Q and collagen domain containing
Amy2a5	53.667	75.667	128.000	6.667	29.333	25.333	2.069	amylase 2a5
Nr4a3	702.200	269.400	744.000	133.400	132.200	143.400	2.069	nuclear receptor subfamily 4, group A, member 3
Rnf223	470.000	236.000	577.000	93.000	123.000	90.000	2.068	ring finger 223
Gm15892	103.500	87.000	129.750	18.750	34.000	24.750	2.047	Predicted gene15892
Gm1564	84.500	1.750	71.750	12.000	5.000	21.250	2.046	Predicted gene1564
Gm14769	55.000	4.000	214.000	10.000	40.000	17.000	2.027	Predicted gene14769
Galr2	258.333	55.667	283.333	62.000	27.333	57.333	2.026	galanin receptor 2
Amer2	96.000	8.000	400.000	35.000	35.000	54.000	2.023	APC membrane recruitment 2
Ltc4s	535.750	1611.500	1423.250	292.000	340.750	248.750	2.018	leukotriene C4 synthase
Klk9	80.000	2.000	1.000	7.500	5.000	8.000	2.017	kallikrein related-peptidase 9
Gm2093	20.500	57.000	54.000	2.000	15.000	15.500	2.017	Predicted gene2093
Apold1	724.000	810.500	920.000	173.000	236.000	201.000	2.009	apolipoprotein L domain containing 1
Serpinb12	420.000	332.250	142.250	1.500	78.250	143.750	2.001	serine (or cysteine) peptidase inhibitor, clade B (ovalbumin), member 12
Gm26785	3.000	7.500	6.500	63.500	113.000	95.500	-4.000	Predicted gene26785
Mro	311.714	133.000	170.000	1267.290	5904.570	2875.710	-4.031	maestro
Cyp11a1	4098.200	4570.200	5019.400	42135.400	91098.400	91192.600	-4.035	cytochrome P450, family 11, subfamily a, polypeptide 1
Wfdc18	82.750	29.250	235.750	714.250	2336.500	2659.500	-4.037	WAP four-disulfide core domain 18
Tmprss4	298.167	60.167	125.333	5830.000	1620.000	542.167	-4.047	transmembrane protease, serine 4
Sctr	4.667	38.333	25.333	912.667	177.333	44.000	-4.053	secretin receptor
Sprr2g	70.000	6.000	18.000	1024.500	381.500	156.000	-4.055	small proline-rich protein 2G
Fgd3	30.750	145.750	69.250	2115.000	1003.500	985.750	-4.062	FYVE, RhoGEF and PH domain containing 3
Ctnna2	37.375	50.250	6.375	148.500	808.375	617.375	-4.066	catenin (cadherin associated protein), alpha 2

5

Biomarkers of mice POF determined by RNA-Seq

Akr1c14	1748.000	964.000	1615.250	26293.500	26816.000	19592.000	-4.070	aldo-keto reductase family 1, member C14
Trpv6	125.000	419.000	464.000	12013.500	4055.500	933.500	-4.076	transient receptor potential cation channel, subfamily V, member 6
Ear2	6.000	5.000	4.000	39.000	115.000	99.500	-4.079	eosinophil-associated, ribonuclease A family, member 2
Gm14017	28.000	4.000	3.000	142.000	295.000	155.000	-4.080	Predicted gene14017
Col5a3	397.667	360.000	863.000	16065.300	6109.330	5625.670	-4.100	collagen, type V, alpha 3
Hsd3b6	128.000	27.000	139.000	236.333	3460.000	1368.330	-4.107	hydroxy-delta-5-steroid dehydrogenase, 3 beta- and steroid delta-isomerase 6
Lrmp	90.636	12.182	7.818	1176.550	635.182	95.909	-4.108	lymphoid-restricted membrane protein
Il1rl1	2.500	10.333	1.000	67.500	73.667	101.167	-4.131	interleukin 1 receptor-like 1
Fndc9	4.000	3.000	1.500	9.500	76.500	63.000	-4.132	fibronectin type III domain containing 9
Gm10340	1.000	0.667	0.667	4.000	18.333	19.333	-4.158	Predicted gene10340
Spc24	65.500	20.000	85.000	1246.500	961.500	884.000	-4.181	SPC24, NDC80 kinetochore complex component, homolog (S. cerevisiae)
Col3a1	7045.250	5832.500	6702.500	195944.000	71532.000	87956.000	-4.182	collagen, type III, alpha 1
Depdc1a	30.500	3.500	4.750	196.500	207.500	303.250	-4.190	DEP domain containing 1a
Aoc1	351.800	320.600	145.000	10412.800	3472.600	1128.400	-4.199	amine oxidase, copper-containing 1
RP23-258M15.6	1.500	0.500	2.500	17.000	52.000	14.500	-4.214	predicted gene 28960
Zfp853	9.500	8.500	3.000	108.000	155.500	130.000	-4.228	zinc finger protein 853
Gm10409	4.000	1.000	0.500	25.000	43.000	36.500	-4.248	Predicted gene10409
Gm3020	2.667	0.667	0.333	16.667	28.333	25.333	-4.262	Predicted gene3020
Inha	4600.500	3228.000	3754.000	34973.500	112793.000	75024.500	-4.266	inhibin alpha
Atf7ip2	3.333	4.000	4.167	27.833	80.167	114.000	-4.271	activating transcription factor 7 interacting protein 2
Entpd8	14.222	0.222	4.778	230.556	83.778	57.889	-4.275	ectonucleoside triphosphate diphosphohydrolase 8
Racgap1	111.533	20.867	48.733	1169.070	1083.530	1287.530	-4.289	Rac GTPase-activating protein 1
Arg1	85.500	171.000	226.000	5198.000	3815.000	429.500	-4.291	arginase, liver
Ank1	31.556	23.556	40.611	630.167	801.722	462.278	-4.307	ankyrin 1, erythroid
Glt8d2	6.000	0.250	3.875	75.375	25.750	99.250	-4.307	glycosyltransferase 8 domain containing 2
Hs3st5	20.500	21.000	5.167	507.667	236.500	185.667	-4.317	heparan sulfate (glucosamine) 3-O-sulfotransferase 5
Gm26892	147.000	198.500	351.000	10055.500	3130.000	700.000	-4.317	Predicted gene26892
Gm23119	13.000	8.000	1.000	148.000	166.000	125.000	-4.319	Predicted gene23119
Spdef	31.167	32.500	48.667	102.000	1323.000	819.333	-4.320	SAM pointed domain containing ets transcription factor
Prap1	45.500	197.000	46.500	3488.500	2128.000	159.000	-4.321	proline-rich acidic protein 1
Gjb2	458.000	229.000	10.000	7474.500	2908.500	3548.500	-4.321	gap junction protein, beta 2
Hsd11b2	1034.500	668.500	859.000	33862.000	5755.000	11662.500	-4.323	hydroxysteroid 11-beta dehydrogenase 2
Trim30b	12.000	0.333	0.333	121.333	80.167	52.333	-4.325	Tripartite motif-containing 30B
Rnf183	4.250	6.750	3.750	205.750	70.750	20.000	-4.329	ring finger protein 183
Spdl1	49.750	7.750	5.500	413.000	458.000	414.500	-4.351	spindle apparatus coiled-coil protein 1
Car12	525.833	157.833	644.833	18904.700	6068.170	2244.670	-4.357	carbonic anhydrase 12
Card11	12.000	1.500	86.000	845.500	549.500	654.500	-4.364	caspase recruitment domain family, member 11
Oas3	64.500	58.500	3.000	1824.000	617.750	177.500	-4.378	2'-5' oligoadenylate synthetase 3
Slfn9	92.000	60.000	106.000	2832.500	933.000	1608.250	-4.380	Schlafen 9
Gm6133	3.000	8.000	6.000	9.000	205.000	141.000	-4.384	Predicted gene6133
Padi4	143.800	109.400	301.600	8263.200	2261.400	1118.400	-4.391	peptidyl arginine deiminase, type IV

Biomarkers of mice POF determined by RNA-Seq

Gm6821	1.000	0.500	4.000	40.000	41.500	34.500	-4.399	Predicted gene6821
Nipal1	46.000	29.000	109.000	798.000	1640.000	1449.000	-4.401	NIPA-like domain containing 1
Jakmip3	56.500	0.750	9.000	156.500	877.500	368.500	-4.404	janus kinase and microtubule interacting protein 3
Tsga10ip	1.000	2.000	8.000	25.500	105.500	102.000	-4.405	testis specific 10 interacting protein
Krt83	108.000	37.000	17.000	2471.500	812.000	189.500	-4.422	Keratin 83
Gabrg3	16.500	1.500	1.000	23.750	201.500	186.750	-4.439	gamma-aminobutyric acid (GABA) A receptor, subunit gamma 3
Gm26641	1.000	7.000	2.000	32.500	75.500	112.000	-4.459	Predicted gene26641
Troap	38.500	46.000	23.000	573.000	975.500	873.000	-4.493	trophinin associated protein
Gm14005	25.750	5.500	68.250	1330.880	729.625	190.500	-4.500	Predicted gene14005
Nkain1	34.500	4.750	5.250	337.500	289.000	393.000	-4.518	Na+/K+ transporting ATPase interacting 1
Col6a4	4068.000	1477.500	3878.500	152924.000	23330.500	42221.800	-4.535	collagen, type VI, alpha 4
Syt16	3.000	7.500	2.500	101.000	129.500	74.500	-4.552	synaptotaPredicted genein XVI
Fbn2	950.000	340.500	580.000	19171.000	10724.000	14050.500	-4.554	Fibrillin 2
Oas2	55.600	136.000	346.000	7663.600	3887.400	1100.400	-4.557	2'-5' oligoadenylate synthetase 2
Bai3	17.417	9.833	13.000	737.500	44.917	170.667	-4.566	adhesion G protein-coupled receptor B3
Gm11417	13.000	1.500	4.500	94.000	280.000	78.500	-4.574	Predicted gene11417
Atad3aos	3.600	1.000	3.000	55.000	34.800	92.600	-4.585	ATPase family, AAA domain containing 3A, opposite strand
Gm22918	8.000	7.000	11.000	72.000	365.000	195.000	-4.603	Predicted gene22918
Gm25287	8.000	7.000	11.000	72.000	365.000	195.000	-4.603	Predicted gene25287
Bcl11b	1.000	2.000	4.750	32.250	68.000	96.500	-4.666	B cell leukemia/lymphoma 11B
Tnni1	5.700	0.200	0.200	13.000	66.900	76.200	-4.678	troponin I, skeletal, slow 1
Col1a1	9107.400	6641.400	9684.200	382271.000	135957.000	134606.000	-4.682	collagen, type I, alpha 1
Pclo	24.167	15.833	37.500	486.667	924.667	587.667	-4.689	piccolo (presynaptic cytomatrix protein)
Glrp1	8.000	8.000	2.500	237.000	115.000	127.500	-4.696	glutamine repeat protein 1
Gm3667	1.500	1.500	2.000	52.000	54.500	23.500	-4.700	Predicted gene3667
Pik3c2g	6.867	0.733	0.133	50.533	71.733	79.000	-4.702	phosphatidylinositol-4-phosphate 3-kinase catalytic subunit type 2 gamma
Cd200r4	2.250	1.000	0.500	11.000	41.750	45.000	-4.704	CD200 receptor 4
Col24a1	26.200	26.200	10.400	1117.400	371.200	166.000	-4.720	collagen, type XXIV, alpha 1
Has2	9.000	22.000	4.000	595.500	176.500	161.500	-4.737	hyaluronan synthase 2
Rab37	38.200	9.600	25.400	221.200	1107.000	644.800	-4.752	RAB37, member RAS oncogene family
Ace2	15.250	12.000	7.500	186.500	333.500	426.250	-4.767	angiotensin I converting enzyme (peptidyl-dipeptidase A) 2
Sfrp4	888.000	383.500	431.000	6000.000	17824.000	23524.000	-4.798	secreted frizzled-related protein 4
Trim15	7.250	7.500	30.750	900.500	324.750	40.250	-4.798	tripartite motif-containing 15
Slc16a14	1.333	3.333	139.000	3183.330	616.667	278.333	-4.827	solute carrier family 16 (monocarboxylic acid transporters), member 14
Myo18b	1.800	3.200	14.800	237.000	213.800	113.600	-4.833	myosin XVIIIb
Col6a3	3607.440	2748.670	3491.440	193789.000	45500.800	45666.700	-4.855	collagen, type VI, alpha 3
Gm12427	132.500	145.000	330.500	845.000	7977.000	8907.500	-4.866	Predicted gene12427
Gabrb3	2.667	1.167	3.167	77.167	36.833	93.167	-4.887	gamma-aminobutyric acid (GABA) A receptor, subunit beta 3
Fam228a	2.500	4.000	3.000	71.500	128.500	84.000	-4.902	family with sequence similarity 228, member A
Gm4787	2.000	2.000	5.000	97.000	100.000	74.000	-4.912	Predicted gene4787
Hrasls	2.600	4.400	0.400	24.200	134.600	65.200	-4.920	HRAS-like suppressor

Biomarkers of mice POF determined by RNA-Seq

Gene							Log FC	Description
Pate2	0.200	0.600	2.200	23.400	32.600	35.400	-4.929	prostate and testis expressed 2
P4ha3	17.200	4.400	59.800	1537.200	631.200	313.400	-4.930	procollagen-proline, 2-oxoglutarate 4-dioxygenase (proline 4-hydroxylase), alpha polypeptide III
Pde11a	3.250	1.750	0.750	35.250	99.750	42.500	-4.948	phosphodiesterase 11A
Ptprt	10.429	27.143	9.000	209.000	545.714	722.429	-4.987	protein tyrosine phosphatase, receptor type, T
Fam184b	18.000	32.500	15.000	1193.500	762.000	148.500	-5.005	family with sequence similarity 184, member B
Sprr2a2	675.000	608.000	549.000	47984.700	9370.000	1496.000	-5.006	Small proline-rich protein 2A2
Ces2b	24.667	9.000	3.000	882.000	167.667	133.333	-5.012	Carboxyesterase 2B
Cdkn3	38.500	6.000	2.000	419.000	581.500	509.000	-5.021	cyclin-dependent kinase inhibitor 3
Gm4779	1.000	2.000	0.750	59.750	44.750	18.500	-5.036	predicted gene 4779
Nrk	45.333	96.667	44.833	5258.000	508.500	469.333	-5.061	Nik related kinase
Gm15218	0.500	1.000	0.500	16.500	15.500	35.000	-5.066	Predicted gene15218
Wnt10b	11.000	36.000	52.667	275.000	1598.000	1476.670	-5.071	wingless-type MMTV integration site family, member 10B
Dsc2	140.600	82.600	175.600	9459.600	2855.600	1200.600	-5.083	desmocollin 2
Aurkb	5.333	23.444	19.111	530.778	490.444	625.111	-5.103	aurora kinase B
BC030870	16.000	2.000	4.500	442.000	242.000	90.000	-5.104	CDNA sequence BC030870
Gm12059	2.000	2.000	4.000	37.500	90.500	156.500	-5.152	Predicted gene12059
Defb19	10.000	68.000	49.000	518.000	2417.000	1692.000	-5.187	defensin beta 19
Hist1h4i	2.000	3.000	4.000	108.000	83.000	139.000	-5.196	histone cluster 1, H4i
Gm15816	5.000	12.000	25.000	538.500	629.000	373.000	-5.197	Predicted gene15816
RP24-217M7.2	6.667	1.833	6.000	95.167	252.333	195.000	-5.225	RIKEN cDNA C430002N11 gene
Dscam	76.000	3.000	55.000	3528.000	814.500	697.500	-5.233	DS cell adhesion molecule
Ryr1	3.000	3.333	0.333	37.000	136.667	82.333	-5.263	ryanodine receptor 1, skeletal muscle
Gm15770	1.000	1.000	1.000	41.000	53.000	23.000	-5.285	Predicted gene15770
Zfp493	3.500	2.500	11.750	151.500	295.250	249.750	-5.294	Zinc finger protein 493
D330050G23Rik	0.500	7.250	0.500	45.000	180.750	99.000	-5.299	RIKEN cDNA D330050G23 gene
Ckmt1	114.727	35.364	125.000	7503.360	2626.450	818.091	-5.315	creatine kinase, mitochondrial 1, ubiquitous
Apol7a	5.000	1.000	11.333	333.333	249.333	110.833	-5.322	Apolipoprotein L 7a
Lect1	116.667	72.833	52.667	1898.330	4369.000	3672.830	-5.359	chondromodulin
Unc5cl	111.000	45.000	92.429	7005.430	3011.710	450.714	-5.397	unc-5 family C-terminal like
Srpx2	44.000	19.000	15.667	860.000	1259.670	1393.000	-5.481	sushi-repeat-containing protein, X-linked 2
Gm5532	3.500	0.500	1.000	56.000	67.000	102.500	-5.495	Predicted gene5532
Slfn4	4.000	15.333	9.000	312.000	596.667	404.000	-5.534	Schlafen 4
Cenpw	1.000	7.000	1.500	97.000	138.000	217.500	-5.574	centromere protein W
Mug-ps1	98.750	6.750	68.750	2683.000	2968.750	2693.250	-5.582	Murinoglobulin, pseudogene 1
Gm15413	9.000	1.000	1.000	155.500	164.000	209.000	-5.586	Predicted gene15413
Crtac1	43.000	51.500	57.500	6027.000	132.000	1219.500	-5.601	cartilage acidic protein 1
Gm6374	2.000	1.000	2.000	77.000	101.000	66.000	-5.609	Predicted gene6374
Bglap3	0.667	0.333	1.000	46.333	22.667	29.000	-5.615	bone gamma-carboxyglutamate protein 3
Lrrtm4	0.111	0.111	1.333	4.444	13.778	58.222	-5.619	leucine rich repeat transmembrane neuronal 4
A2m	790.500	540.000	332.500	66443.500	1593.000	17763.500	-5.689	alpha-2-macroglobulin

8

Biomarkers of mice POF determined by RNA-Seq

Fsbp	4.000	2.000	2.000	104.500	151.500	161.000	-5.704	fibrinogen silencer binding protein
Ngfr	367.000	202.500	341.000	37244.500	5163.000	7376.000	-5.773	nerve growth factor receptor (TNFR superfamily, member 16)
Dscc1	8.000	3.000	1.000	218.000	174.500	278.000	-5.804	DNA replication and sister chromatid cohesion 1
Hsd17b1	147.000	122.000	76.500	1992.000	11364.500	6226.000	-5.825	hydroxysteroid (17-beta) dehydrogenase 1
Trim36	2.667	13.000	5.667	646.000	284.333	281.667	-5.828	tripartite motif-containing 36
Nr5a2	293.000	78.000	377.333	6575.670	21476.000	16532.700	-5.897	nuclear receptor subfamily 5, group A, member 2
Mogat2	0.667	7.333	3.333	254.000	240.000	194.333	-5.924	monoacylglycerol O-acyltransferase 2
Spink10	0.286	0.143	2.571	50.143	92.857	47.000	-5.985	serine peptidase inhibitor, Kazal type 10
Galnt13	5.667	6.500	0.500	600.333	169.333	46.667	-6.010	polypeptide N-acetylgalactosaminyltransferase 13
Mug2	2.000	6.000	209.000	5256.500	4024.000	4795.500	-6.019	Murinoglobulin 2
Eya4	0.333	0.667	2.000	69.667	75.667	67.667	-6.150	EYA transcriptional coactivator and phosphatase 4
Chst8	32.000	19.250	47.750	2630.500	2782.750	1978.000	-6.222	Carbohydrate (N-acetylgalactosamine 4-0) sulfotransferase 8
Gm16277	2.000	1.500	4.000	358.500	179.000	64.500	-6.327	Predicted gene 16277
Fer1l4	6.000	2.571	25.000	1743.430	942.571	81.429	-6.365	Fer-1-like 4 (C. elegans)
Muc4	130.000	137.667	249.333	40051.100	7156.890	2589.000	-6.590	Mucin 4, cell surface associated
Cyp17a1	141.500	84.500	29.500	5418.000	8416.000	11347.000	-6.623	Cytochrome P450, family 17, subfamily A, polypeptide 1
Add2	5.000	2.000	45.500	4380.500	881.000	176.500	-6.695	Adducin 2 (beta)
Gm13032	249.000	218.000	183.000	46115.000	19705.000	2436.500	-6.714	Predicted gene 13032
Nppc	7.000	4.000	28.000	2306.000	1147.500	710.000	-6.738	Natriuretic peptide type C
Gm13031	144.500	132.500	91.500	29791.500	8219.000	1335.000	-6.738	Predicted gene 13031
Padi2	200.750	189.000	197.000	57470.500	12099.800	2317.250	-6.937	Peptidyl arginine deiminase, type II
Padi1	406.000	762.500	823.500	181334.000	54786.500	9252.000	-6.945	Peptidyl arginine deiminase, type I
Gm12248	31.000	1.000	22.500	7465.500	1088.500	230.500	-7.333	Predicted gene 12248
Inhba	14.333	15.667	166.667	3655.670	25519.000	9380.670	-7.615	Inhibin, beta A
Apoa1	6.667	1.333	2.000	260.667	915.667	786.333	-7.617	Apolipoprotein A-I
Ptpn5	5.500	18.917	37.250	7371.920	4995.750	2465.830	-7.910	Protein tyrosine phosphatase, non-receptor type 5
Hba-a1	60.667	11.000	36.000	9740.330	9518.330	8549.000	-8.013	Hemoglobin alpha, adult chain 1
Hba-a2	61.333	7.000	33.000	9944.330	9843.330	8709.330	-8.136	Hemoglobin alpha, adult chain 2
Hbb-bt	21.000	14.000	2.000	4490.000	3878.000	3544.000	-8.331	Hemoglobin, beta adult major chain
Hbb-bs	19.500	15.250	2.000	5226.750	4485.250	4400.750	-8.585	Hemoglobin, beta adult minor chain
Sprr2f	13.000	6.000	8.000	31219.500	12000.500	700.500	-10.668	Small proline-rich protein 2F

Table S2. GO analysis

Category	Term	Count	P Value	Regulation
GO_CC	GO:0005886~plasma membrane	199	2.45E-04	Up
GO_CC	GO:0005576~extracellular region	127	1.02E-04	Up
GO_CC	GO:0044459~plasma membrane part	110	0.015511942	Up
GO_CC	GO:0044421~extracellular region part	65	5.63E-04	Up
GO_CC	GO:0000267~cell fraction	54	3.17E-04	Up
GO_CC	GO:0005615~extracellular space	49	1.74E-04	Up
GO_CC	GO:0005626~insoluble fraction	47	0.001195315	Up
GO_CC	GO:0005624~membrane fraction	45	0.001832291	Up
GO_CC	GO:0005829~cytosol	42	0.026639991	Up
GO_CC	GO:0031226~intrinsic to plasma membrane	41	0.042493314	Up
GO_CC	GO:0019898~extrinsic to membrane	37	0.02750463	Up
GO_CC	GO:0030054~cell junction	36	0.040070863	Up
GO_CC	GO:0005792~microsome	26	1.09E-05	Up
GO_CC	GO:0042598~vesicular fraction	26	1.96E-05	Up
GO_CC	GO:0043005~neuron projection	22	0.028104318	Up
GO_MF	GO:0043167~ion binding	279	2.58E-05	Up
GO_MF	GO:0043169~cation binding	276	2.63E-05	Up
GO_MF	GO:0046872~metal ion binding	275	1.82E-05	Up
GO_MF	GO:0046914~transition metal ion binding	183	0.002241743	Up
GO_MF	GO:0008270~zinc ion binding	140	0.043968863	Up
GO_MF	GO:0003677~DNA binding	130	0.003106259	Up
GO_MF	GO:0030528~transcription regulator activity	105	1.65E-05	Up
GO_MF	GO:0003700~transcription factor activity	72	6.79E-05	Up
GO_MF	GO:0043565~sequence-specific DNA binding	48	0.005430357	Up
GO_MF	GO:0000287~magnesium ion binding	38	0.004477108	Up
GO_MF	GO:0005506~iron ion binding	36	7.48E-04	Up
GO_MF	GO:0030246~carbohydrate binding	33	0.0014787	Up
GO_MF	GO:0046983~protein dimerization activity	33	0.00442097	Up
GO_MF	GO:0009055~electron carrier activity	26	2.55E-04	Up
GO_MF	GO:0004857~enzyme inhibitor activity	25	0.00713273	Up
GO_MF	GO:0048037~cofactor binding	24	0.005849552	Up
GO_MF	GO:0016563~transcription activator activity	23	0.045064432	Up
GO_MF	GO:0030247~polysaccharide binding	21	4.26E-05	Up
GO_MF	GO:0001871~pattern binding	21	4.26E-05	Up
GO_BP	GO:0045449~regulation of transcription	164	0.001570933	Up
GO_BP	GO:0006350~transcription	139	3.23E-04	Up
GO_BP	GO:0051252~regulation of RNA metabolic process	112	0.005438227	Up
GO_BP	GO:0006355~regulation of transcription, DNA-dependent	111	0.004718602	Up
GO_BP	GO:0007242~intracellular signaling cascade	74	0.005095364	Up
GO_BP	GO:0006811~ion transport	63	0.001345501	Up
GO_BP	GO:0055114~oxidation reduction	59	0.002316868	Up
GO_BP	GO:0010604~positive regulation of macromolecule metabolic process	54	0.006430611	Up
GO_BP	GO:0006357~regulation of transcription from RNA polymerase II promoter	50	0.020802149	Up
GO_BP	GO:0009891~positive regulation of biosynthetic process	49	0.005479497	Up
GO_BP	GO:0031328~positive regulation of cellular biosynthetic process	48	0.007426869	Up
GO_BP	GO:0043009~chordate embryonic development	46	8.35E-05	Up
GO_BP	GO:0009792~embryonic development ending in birth or egg hatching	46	1.04E-04	Up
GO_BP	GO:0010628~positive regulation of gene expression	46	0.002016063	Up
GO_BP	GO:0010033~response to organic substance	46	0.003854507	Up
GO_BP	GO:0010557~positive regulation of macromolecule biosynthetic process	46	0.009281006	Up
GO_BP	GO:0045941~positive regulation of transcription	45	0.002070929	Up
GO_BP	GO:0045935~positive regulation of nucleobase, nucleoside, nucleotide and nucleic acid metabolic process	45	0.007489017	Up
GO_BP	GO:0051173~positive regulation of nitrogen compound metabolic process	45	0.012759829	Up
GO_CC	GO:0005623~cell	1365	0.003643	Down
GO_CC	GO:0044464~cell part	1362	0.004018	Down

Biomarkers of mice POF determined by RNA-Seq

GO_CC	GO:0005576~extracellular region	491	1.60E-11	Down
GO_CC	GO:0044421~extracellular region part	465	1.77E-09	Down
GO_CC	GO:0071944~cell periphery	429	8.86E-06	Down
GO_CC	GO:0005886~plasma membrane	415	9.90E-06	Down
GO_CC	GO:0031982~vesicle	375	0.006008	Down
GO_CC	GO:0031988~membrane-bounded vesicle	368	0.002436	Down
GO_CC	GO:0043234~protein complex	360	0.014521	Down
GO_CC	GO:0043228~non-membrane-bounded organelle	334	0.022316	Down
GO_CC	GO:0043232~intracellular non-membrane-bounded organelle	334	0.022316	Down
GO_CC	GO:1903561~extracellular vesicle	323	8.56E-04	Down
GO_CC	GO:0043230~extracellular organelle	323	0.001004	Down
GO_CC	GO:0070062~extracellular exosome	322	7.61E-04	Down
GO_CC	GO:0065010~extracellular membrane-bounded organelle	322	8.94E-04	Down
GO_CC	GO:0044459~plasma membrane part	265	1.45E-07	Down
GO_CC	GO:0005615~extracellular space	195	2.24E-11	Down
GO_CC	GO:0031226~intrinsic component of plasma membrane	146	0.002241	Down
GO_CC	GO:0005887~integral component of plasma membrane	138	0.002321	Down
GO_CC	GO:0005694~chromosome	120	4.23E-08	Down
GO_CC	GO:0009986~cell surface	113	1.90E-06	Down
GO_CC	GO:0044427~chromosomal part	112	1.59E-07	Down
GO_MF	GO:0003824~catalytic activity	445	0.006391	Down
GO_MF	GO:0016787~hydrolase activity	193	0.026339	Down
GO_MF	GO:0043167~ion binding	159	0.005827	Down
GO_MF	GO:0005102~receptor binding	143	0.006102	Down
GO_MF	GO:0044877~macromolecular complex binding	131	0.035432	Down
GO_MF	GO:0005215~transporter activity	126	2.37E-05	Down
GO_MF	GO:0022892~substrate-specific transporter activity	119	5.16E-06	Down
GO_MF	GO:0022857~transmembrane transporter activity	107	3.75E-05	Down
GO_MF	GO:0043168~anion binding	107	0.03983	Down
GO_MF	GO:0098772~molecular function regulator	104	0.022642	Down
GO_MF	GO:0022891~substrate-specific transmembrane transporter activity	101	2.47E-05	Down
GO_MF	GO:0015075~ion transmembrane transporter activity	95	2.45E-05	Down
GO_MF	GO:0032403~protein complex binding	85	0.002613	Down
GO_MF	GO:0097367~carbohydrate derivative binding	83	0.007141	Down
GO_MF	GO:0036094~small molecule binding	81	0.021772	Down
GO_MF	GO:0043169~cation binding	79	0.006684	Down
GO_MF	GO:0030234~enzyme regulator activity	79	0.028894	Down
GO_MF	GO:0016491~oxidoreductase activity	76	0.001711	Down
GO_MF	GO:0008324~cation transmembrane transporter activity	71	1.63E-04	Down
GO_MF	GO:0046872~metal ion binding	70	0.014529	Down
GO_BP	GO:0044699~single-organism process	1253	0.037518	Down
GO_BP	GO:0044707~single-multicellular organism process	570	0.002169	Down
GO_BP	GO:0051179~localization	493	0.019535	Down
GO_BP	GO:0051234~establishment of localization	387	0.003149	Down
GO_BP	GO:1902578~single-organism localization	375	3.23E-04	Down
GO_BP	GO:0006810~transport	366	0.006531	Down
GO_BP	GO:0044765~single-organism transport	350	6.75E-04	Down
GO_BP	GO:0048513~animal organ development	336	0.022582	Down
GO_BP	GO:0065008~regulation of biological quality	322	0.003758	Down
GO_BP	GO:0006950~response to stress	321	0.001595	Down
GO_BP	GO:0051239~regulation of multicellular organismal process	274	0.015742	Down
GO_BP	GO:0006793~phosphorus metabolic process	270	0.033721	Down
GO_BP	GO:0006796~phosphate-containing compound metabolic process	267	0.031026	Down
GO_BP	GO:0002376~immune system process	258	1.70E-05	Down
GO_BP	GO:0010033~response to organic substance	242	0.007704	Down
GO_BP	GO:0070887~cellular response to chemical stimulus	226	0.010436	Down
GO_BP	GO:0043933~macromolecular complex subunit organization	226	0.021123	Down
GO_BP	GO:0009605~response to external stimulus	216	4.73E-04	Down

Table S3. KEGG Pathway

Term	Count	P Value	Regulation
Mmu04080: Neuroactive ligand-receptor interaction	26	0.014431735	Up
Mmu00982: Drug metabolism	20	6.02E-08	Up
Mmu04920: Adipocytokine signaling pathway	15	3.73E-05	Up
Mmu03320: PPAR signaling pathway	14	8.43E-04	Up
Mmu00980: Metabolism of xenobiotics by cytochrome P450	13	5.26E-04	Up
Mmu04115: p53 signaling pathway	13	7.99E-04	Up
Mmu04070: Phosphatidylinositol signaling system	10	0.037004146	Up
Mmu04710: Circadian rhythm	8	3.62E-06	Up
Mmu00480: Glutathione metabolism	8	0.036516589	Up
Mmu00330: Arginine and proline metabolism	8	0.03997015	Up
Mmu00562: Inositol phosphate metabolism	8	0.043630308	Up
Mmu00380: Tryptophan metabolism	7	0.032217305	Up
Mmu04960: Aldosterone-regulated sodium reabsorption	7	0.039806882	Up
Mmu00250: Alanine, aspartate and glutamate metabolism	6	0.032786105	Up
Mmu01100: Metabolic pathways	163	0.005692	Down
Mmu05034: Alcoholism	51	2.18E-09	Down
Mmu04080: Neuroactive ligand-receptor interaction	50	1.86E-04	Down
Mmu05322: Systemic lupus erythematosus	49	8.33E-14	Down
Mmu04060: Cytokine-cytokine receptor interaction	46	4.27E-04	Down
Mmu05203: Viral carcinogenesis	38	0.010025	Down
Mmu04974: Protein digestion and absorption	30	4.13E-09	Down
Mmu04020: Calcium signaling pathway	28	0.025895	Down
Mmu04110: Cell cycle	26	5.04E-04	Down
Mmu04512: ECM-receptor interaction	22	3.24E-05	Down
Mmu05146: Amoebiasis	20	0.011504	Down
Mmu00240: Pyrimidine metabolism	19	0.01175	Down
Mmu04064: NF-kappa B signaling pathway	19	0.01175	Down
Mmu05145: Toxoplasmosis	19	0.02678	Down
Mmu04640: Hematopoietic cell lineage	18	0.004246	Down
Mmu04612: Antigen processing and presentation	18	0.011941	Down
Mmu00140: Steroid hormone biosynthesis	16	0.01862	Down
Mmu04727: GABAergic synapse	16	0.022757	Down
Mmu04913: Ovarian steroidogenesis	15	7.59E-04	Down
Mmu04260: Cardiac muscle contraction	15	0.018886	Down
Mmu03320: PPAR signaling pathway	14	0.046826	Down
Mmu05330: Allograft rejection	13	0.036557	Down
Mmu05412: Arrhythmogenic right ventricular cardiomyopathy (ARVC)	13	0.044434	Down
Mmu05143: African trypanosomiasis	12	2.69E-04	Down
Mmu05340: Primary immunodeficiency	12	2.69E-04	Down
Mmu00330: Arginine and proline metabolism	12	0.004865	Down
Mmu04672: Intestinal immune network for IgA production	11	0.004958	Down
Mmu05144: Malaria	11	0.013465	Down
Mmu04614: Renin-angiotensin system	10	0.002551	Down
Mmu04975: Fat digestion and absorption	10	0.007251	Down
Mmu05150: Staphylococcus aureus infection	10	0.048005	Down
Mmu05310: Asthma	9	9.25E-04	Down
Mmu03030: DNA replication	9	0.008784	Down
Mmu00100: Steroid biosynthesis	8	3.89E-04	Down
Mmu00670: One carbon pool by folate	7	0.002294	Down
Mmu04977: Vitamin digestion and absorption	7	0.00986	Down
Mmu04744: Phototransduction	7	0.015557	Down
Mmu00900: Terpenoid backbone biosynthesis	6	0.034747	Down